We are IntechOpen,
the world's leading publisher of
Open Access books
Built by scientists, for scientists

6,900
Open access books available

185,000
International authors and editors

200M
Downloads

154
Countries delivered to

Our authors are among the

TOP 1%
most cited scientists

12.2%
Contributors from top 500 universities

CLARIVATE ANALYTICS

BOOK CITATION INDEX

INDEXED

WEB OF SCIENCE™

Selection of our books indexed in the Book Citation Index
in Web of Science™ Core Collection (BKCI)

Interested in publishing with us?
Contact book.department@intechopen.com

Numbers displayed above are based on latest data collected.
For more information visit www.intechopen.com

Heat Transfer in Molecular Crystals

V.A. Konstantinov

B. Verkin Institute for Low Temperature Physics and Engineering
of the National Academy of Sciences of Ukraine, Kharkov
Ukraine

1. Introduction

This short review does not pretend to comprehend all available information concerning the thermal conductivity of molecular crystals, in particular, at low temperatures (below 20*K*). For such kind of information see, for example, Batchelder, 1977; Gorodilov et al., 2000; Jezowski et al., 1997; Ross et al., 1974; Stachowiak et al., 1994. The goal of this paper consists in presentation and generalization of the new experimental results and theoretical models, accumulated over the past 2-3 decades, to a certain extent changing existing view about the heat transfer in crystals. Quite recently, it was not doubted that high-temperature thermal conductivity of molecular crystals is proportional to the inverse temperature, $\Lambda \propto 1/T$. It was based on both the experimental data and assumptions being evident at first sight from which this dependence followed. In simple kinetic model, the phonon thermal conductivity can be represented as $\Lambda = 1/3Cvl$, where C (the heat capacity) and v (the sound velocity) can be considered to be constant at $T \geq \Theta_D$, and averaged phonon mean-free path l is inversely proportional to the temperature. More precise expression (see, for example, Berman, 1976; Slack, 1979) can be written in the form:

$$\Lambda = K\frac{ma\Theta_D^3}{\gamma^2 T} \, , \qquad (1)$$

where m is the average atomic (molecular) mass; a^3 is the volume per atom (molecule); $\gamma = -(\partial ln\Theta_D / \partial lnV)_T$ is the Grüneisen parameter, and K is a structure factor. In time, data on the deviation from $1/T$ dependence has accumulated, and in a number of cases some ideas qualitatively explaining the observed behaviour of thermal conductivity have been proposed. The problem has been, however, that the theory predicts the $1/T$ law at the constant volume of the sample, whereas the measurements were carried out at constant pressure. In this case, thermal expansion, been usually rather essential at high temperatures (the molar volume of molecular crystals may change up to 10-20% in the temperature interval from zero and up to the melting temperature) leads, as a rule, to additional decrease of Λ with rise of temperature. Moreover, in many cases, the phonons are not the only excitations determining the heat transfer and scattering process. The dependence of the thermal conductivity on the molar volume can be described using Bridgman's coefficient:

$$g = -\left(\partial ln\Lambda / \partial lnV\right)_T \, , \qquad (2)$$

It follows from Eqs. (1) and (2) that for crystals:

$$g = 3\gamma + 2q - 1/3 , \tag{3}$$

were $q=(\partial \ln\gamma/\partial \ln V)_T$. Ordinarily, it is assumed that $\gamma \propto V$ and the second Grüneisen coefficient $q \cong 1$ (Slack, 1979; Ross et al., 1984). Taking into account that $\gamma \cong 2 \div 3$ for a number of simple molecular crystals (Manzhelii et al., 1997) it is expected that $g \cong 8 \div 11$ and $\Lambda \propto V^{8 \div 11}$. It means that 1% change in volume may result in 8-11% change in thermal conductivity. Data measured at saturated vapour and atmosphere pressures can be considered as equivalent because the difference between them is much smaller than accuracy of experiment and they will be further denoted as isobaric ($P \cong 0$, MPa) data.

Constant-volume investigations are possible for molecular solids having a comparatively large compressibility coefficient. Using a high-pressure cell, it is possible to grow a solid sample of sufficient density. In subsequent experiments it can be cooled with practically unchanged volume, while the pressure in the cell decreases. In samples of moderate densities the pressure drops to zero at a certain characteristic temperature T_0 and the isochoric condition is then broken; on further cooling, the sample can separate from the walls of the cell. In the case of a fixed volume, melting of the sample occurs in a certain temperature interval and its onset shifts towards higher temperatures as density of samples increases (For more experimental details see Konstantinov et al., 1999).

As the temperature increases, phonon scattering processes intensify, the mean-free path length l decreases and it may approach to the lattice parameter. The question of what occurs when the phonon mean-free path becomes comparable to the lattice parameter or its own wavelength is one of the most intriguing problems in the thermal conductivity of solids (see, for example, Auerbach & Allen, 1984; Feldman et al., 1993; Sheng et al., 1994). According to preferably accepted standpoint, in this case the vibrational modes assume a "diffusive" character, but the basic features of the kinetic approach retain their validity. Some progress in the description of the heat transport in strongly disordered materials has come about through the concept of the minimum thermal conductivity Λ_{min} (Slack, 1979; Cahill et al., 1992), which is based on the picture where the lower limit of the thermal conductivity is reached when the heat is being transported through a random walk of the thermal energy between the neighboring atoms or molecules vibrating with random phases. In this case Λ_{min} can be written as the following sum of three Debye integrals:

$$\Lambda_{min} = \left(\frac{\pi}{6}\right)^{1/3} k_B \, n^{2/3} \sum_i v_i \left\{ \left(\frac{T}{\Theta_i}\right)^2 \int_0^{\Theta_i/T} \frac{x^3 e^x}{\left(e^x - 1\right)^2} dx \right\} , \tag{4}$$

The summation is taken over three (two transverse and one longitudinal) sound modes with the sound speeds v_i; Θ_i is the Debye cutoff frequency for each polarization expressed in degrees K; $\Theta_i = v_i \left(\hbar/k_B\right) \left(6\pi^2 n\right)^{1/3}$; n is the number density of atoms or molecules. Although no theoretical justification exists as yet for this picture of the heat transport, the evidence for its validity has been obtained on a number of amorphous solids in which the high temperature thermal conductivity has been found to agree with the value predicted by this model. Indirect evidence has also been obtained in measurements of the thermal conductivity of highly disordered crystalline solids, in which no thermal conductivity

smaller than that predicted by this model seems to have ever been observed (Cahill et al., 1992). It is evident, that thermal conductivity approaches its lower limit Λ_{min} in amorphous solids and strongly disordered crystals (Auerbach & Allen, 1984; Cahill et al., 1992; Sheng et al., 1994). This raises the question whether or not the three-phonon scattering processes in themselves may result in Λ_{min} in perfect crystals with rise of temperature.
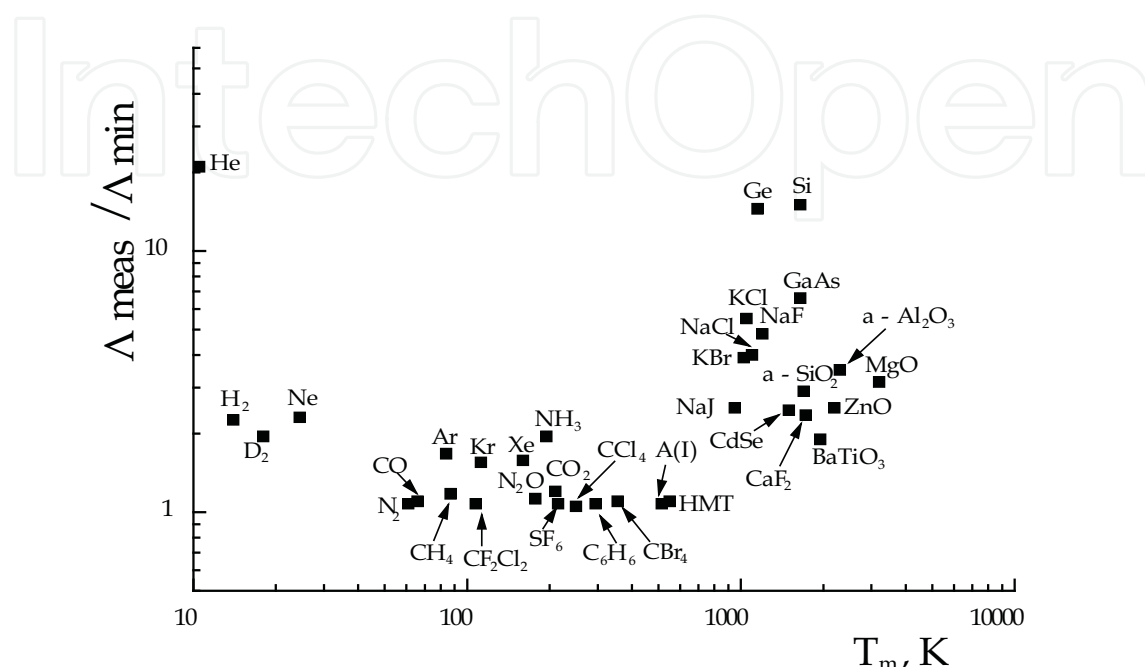

Fig. 1. The ratio $\Lambda_{meas}/\Lambda_{min}$ immediately below the corresponding melting temperatures (T_m) versus T_m for crystals with different types of chemical bonds.

To find an answer let us compare the measured thermal conductivity Λ_{meas} of a number of crystals with different types of chemical bonds and the lower limit to thermal conductivity Λ_{min} at the corresponding melting temperatures T_m (see Fig. 1). It is evident that the ratio $\Lambda_{meas}/\Lambda_{min}$ increases as the crystal bond becomes stronger. In van-der-Waals-type crystals $\Lambda_{meas}/\Lambda_{min} \cong 1.5 \div 2$, while in the crystals with diamond-type structure it is of the order of $10 \div 20$, i.e. van-der-Waals-type crystals are the most suitable objects for observing the thermal conductivity "minimum" due to umklapp processes only and this will be demonstrated further.

Crystals containing molecules or molecular ions are more complicated than crystals containing only atoms and ions, since the former possess translational, orientational and intramolecular degrees of freedom. An important common feature of simple molecular crystals is that in the condensed phases the intermolecular forces are much weaker than the intramolecular ones, so that the molecular parameters remain close to those in the gas. As a rule, the intramolecular forces and associated intramolecular vibration frequencies ($\sim 1000 cm^{-1}$) exceed by an order of magnitude the intermolecular ones (the corresponding lattice-mode frequencies are below $\sim 1000 cm^{-1}$). Such a large difference between the two types of frequencies makes it possible to safely regard the respective types of motion as independent. So as far as the lattice vibrations are concerned, the molecules can be treated as rigid bodies. In such an approximation each molecule participates in two types of

motion: translational, when the molecular center of mass shifts, and rotational, when the center of mass rests. Many features in the dynamics of the simple molecular solids are related to the rotational motion of the molecules (Parsonage & Stavaley, 1972). At very low temperature, the structure of a crystal is perfectly ordered and the molecules can perform only small amplitude translational vibrations at the lattice sites and oscillations around selected axes (libration) in a manner so that the motion of neighboring molecules is correlated and collective translational and orientational excitations (phonons and librons) propagate throw the crystal. Calculation of anharmonic effects show that translational vibrations are characterized by relatively small amplitudes while the amplitude of librational vibrations in molecular crystals is sufficiently large even at $T \cong 0$, so that the harmonic theory can hardly claim to give more than qualitative picture of the librational motion (Briels et al., 1985; Manzhelii et al., 1997). As the temperature increases, the rotational motion may, in principle, pass through the following stages depending on the relationship between the central and anisotropic forces: enlargement of the libration amplitudes, the appearance of jump-like reorientations of the molecules, increase of the frequency of reorientations, hindered rotation of the molecules, and, finally, nearly free rotation of the molecules. In the last two cases a phase transition takes place, as a rule, before the crystal melts, giving rise to a structure in which translational long-range order is preserved while the orientational order is lost. It is a characteristic property of crystals consisting of high-symmetry "globular" molecules like CH_4, N_2, adamantane ($C_{10}H_{16}$) or, in some degree, of "cylindrical" molecules like benzene, C_2F_6 or long-chain n-alkanes. They form high-temperature "plastic" or orientationally-disordered (commonly called ODIC: Orientational Disorder In Crystals) phases in which the rotational motion of molecules resembles their motion in the liquid state (Parsonage & Stavaley, 1972). In crystals consisting of molecules of a lower symmetry the long-range orientational order is preserved, as a rule, up to the melting points.

In harmonic approximation, phonons and librons (rotational excitations) are treated as independent entities. Real phonons are, however, coupled together and with rotational excitations by anharmonic terms of the crystal Hamiltonian (Manzhelii et al., 1997; Lynden-Bell & Michel, 1994). Therefore, translational and orientational types of motions in molecular crystals are not independent of one another, but rather they occur as coupled translational-orientational vibrations. That involves considerable difficulties to describe this case with analytical expressions. As a consequence, a simplified model where the translational and orientational subsystems are described independently is usually used (Manzhelii et al., 1997; Kokshenev et al., 1997). The coupling produces a shift of phonons frequency with respect to the harmonic value as well as a broadening of bands, associated to the finite phonon lifetime. In such approximation the TO coupling results in an additional contribution to the thermal resistance of the crystal $W=1/\Lambda$. This additional thermal resistance may decrease if the frequency of reorientations becomes sufficiently large, so that the TO coupling reduces. The relative simplicity of the investigated molecular crystals made possible an appropriate theoretical interpretation and provided establishing of the general relationships in heat transfer that result from the presence of rotational degrees of freedom of the molecules. In the experimental part of the paper the results of study of isochoric thermal conductivity of solidified inert gases, simple molecular crystals and their solutions at $T \geq \Theta_D$ will be considered then the models intended to explain temperature and volume dependences of thermal conductivity will be discussed.

2. Experimental results.

2.1 The solidified inert gases

The solidified inert gases *Ar*, *Kr* and *Xe* are convenient object for comparison of experimental data with theoretical calculations of thermal conductivity of a lattice since they are simplest solids closely conformable to theoretical models. This fact stimulated a considerable number of experimental and theoretical works (see, for example, the review of Batchelder, 1977). At $T \geq \Theta_D$ the phonon-phonon interaction is the only mechanism, which determines the magnitude and temperature dependence of the thermal conductivity Λ in perfect crystals. If the scattering is not too strong and the picture of elastic waves can be used, theory predicts the thermal conductivity $\Lambda \propto 1/T$ at fixed volume of the sample (Berman, 1976). The more rapid decrease of the thermal conductivity as $\Lambda \propto 1/T^2$ observed in these inert gases under saturated vapour pressure was originally ascribed to scattering process with participation of four or more phonons (Krupski et al., 1968). Later, Slack, 1972 suggested that the change of crystal volume with temperature by itself may lead to considerable deviations from the dependence $\Lambda \propto 1/T$ because of a "quasi-harmonic" change of the spectrum of vibrational modes, and Ecsedy & Klemens, 1977 showed theoretically that four-phonon processes are expected to be weak even at premelting temperatures. Subsequent thermal conductivity studies of solid *Ar*, *Kr* and *Xe* at fixed density (Clayton & Batchelder, 1973; Bondarenko et al., 1982; Konstantinov et al., 1988) confirmed that roughly the dependence $\Lambda \propto 1/T$ is valid when $T \geq \Theta_D$. Fig. 2 shows both isochoric for samples of different densities (Clayton & Batchelder, 1973) and measured under saturated vapour pressure $P \cong 0, MPa$, (Krupski et al., 1968) experimental data for solid argon in the *W* versus *T*
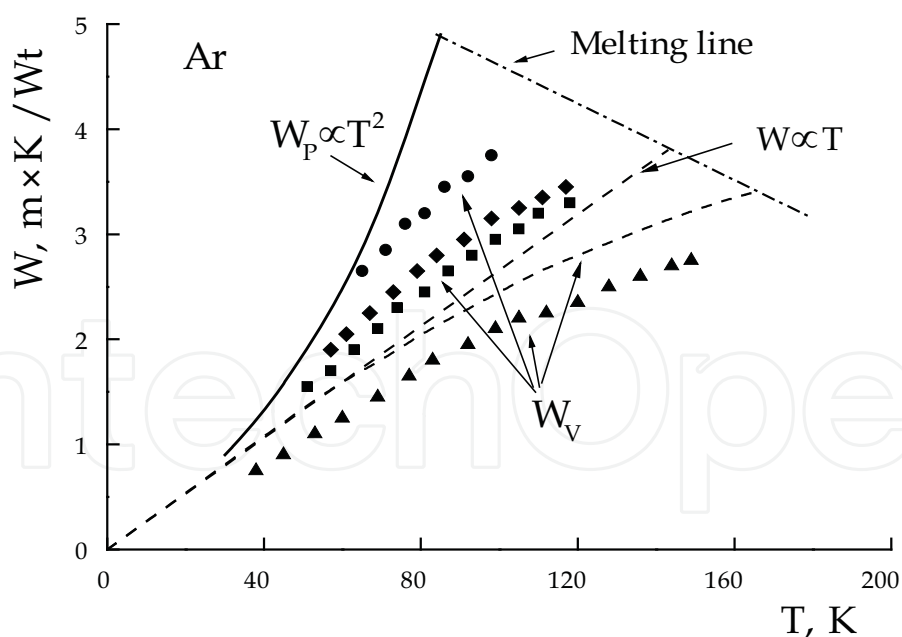

Fig. 2. Isobaric W_P (Krupski et al., 1968) and isochoric W_V (Clayton et al., 1973) thermal resistance $W=1/\Lambda$ of crystalline argon for samples of different densities.

coordinates, where $W=1/\Lambda$ is the thermal resistance of crystal. It is seen that appreciable deviations are observed at the highest temperatures, with the isochoric thermal conductivity varying markedly more slowly than $\Lambda \propto 1/T$ or $W \propto T$ dependence. A similar behaviour was

also observed for krypton (Bondarenko et al., 1982) and xenon (Konstantinov et al., 1988). It was found that Λ can be described by the expression

$$\Lambda = (A/T + B)(V_0/V)^g , \qquad (5)$$

where A and B are constants independent on the temperature; V_0 is molar volume at $T=0K$, and V is actual molar volume $V=V(T)$. The Bridgman's coefficients g for Ar, Kr and Xe were found in good agreement with calculated by Eq. 3 and they are equal to 9.7, 9.4 and 9.2 correspondingly.

The deviations observed were primary attributed to anharmonic renormalisation of the law of phonon dispersion at a fixed volume (Konstantinov et al., 1988). The quantitative calculation has not yet been carried out because of the complexity of model proposed. Later on the thermal conductivity of solid Ar, Kr and Xe was calculated within framework of the Debye model which allows for the fact that the mean-free path of phonons cannot become smaller than half the phonon wavelength (Konstantinov, 2001a).

2.2 Nitrogen-type crystals and oxygen

The N_2–type crystals (N_2, CO, N_2O and CO_2) consisting of linear molecules have rather simple and largely similar physical properties. In these crystals the anisotropic part of the molecular interaction is determined mostly by the electric-quadrupole forces. At low temperatures and pressures, these crystals have a cubic lattice with four molecules per unit cell. The axes of the molecules are along the body diagonals of the cube. In N_2 and CO_2 having equivalent diagonal directions the crystal symmetry is $Pa3$, for the noncentrosymmetrical molecules CO and N_2O the crystal symmetry is $P2_13$. In CO_2 and N_2O the anisotropic interaction is so strong that the crystals melt before the complete orientational disorder occurs. In N_2 and CO the barriers impeding the rotation of the molecules are an order of magnitude lower; as a result, the orientational disordering phase transitions occur at 35.7 and 68.13K, respectively. In the high-temperature phases, N_2 and CO molecules occupy the sites of the HCP lattice of the spatial group $P6_3/mmc$.
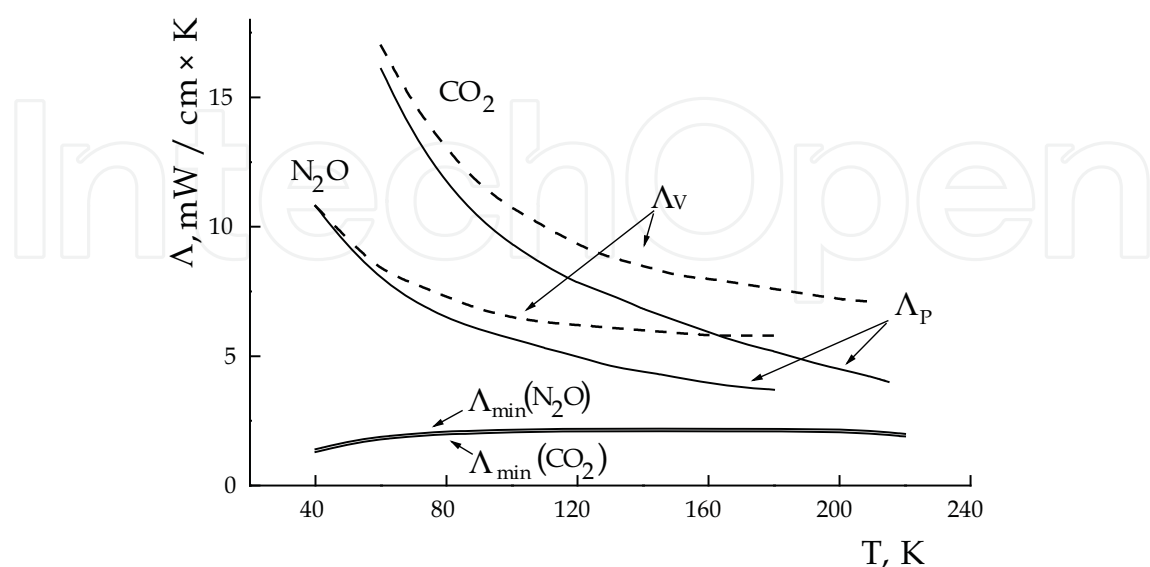

Fig. 3. Isochoric (dashed lines) and isobaric (solid lines) thermal conductivities Λ of CO_2 and N_2O.

The thermal conductivity of solid CO_2, N_2O, N_2 and CO was studied at saturated vapor pressure by Manzhelii et al., 1975. Isochoric thermal conductivity of CO_2 and N_2O was studied by Konstantinov et al., 1988b, and N_2 and CO by Konstantinov et al., 2005b; 2006a. The data for CO_2 and N_2O is shown in Fig. 3, solid and dashed lines depict isobaric and isochoric thermal conductivity respectively. The isochoric thermal conductivity is recalculated to the molar volumes which CO_2 and N_2O have at zero temperature and pressure. The lower limits to thermal conductivity, calculated accordingly to Eq. 4 are shown at the bottom. The Bridgman's coefficients g for nitrogen-type crystals were found in poor agreement with calculated by Eq. 3. The reason for it will be discussed later.

Whereas isobaric thermal conductivity of CO_2 roughly follows $1/T$ dependence, isochoric one deviates rather more strongly from the above dependence than in solidified inert gases. In N_2O both isochoric and isobaric thermal conductivities deviates strongly from $1/T$ dependence. To reveal the features to be associated with the anisotropic component of the molecular interaction it is necessary to compare molecular crystals with rare-gas solids in the reduced coordinates (de Bour, 1948). Such a comparison is of interest for the following reasons: the thermal resistance W_{ph-ph} of an ideal crystal of an inert gas is due solely to phonon-phonon scattering. In CO_2 an additional phonon thermal resistance W_{ph-lib} (or W_{ph-rot}) appears due to interaction phonons with librons (rotational excitations). In the case of N_2O the scattering resulting from dipole disordering is added to these phonon scattering mechanisms (W_{dip}). To a first approximation the total thermal resistance W is:

$$W = W_{ph-ph} + W_{ph-rot} + W_{dip} \qquad (6)$$

It is convenient to make a comparison between the crystals mentioned because all of them have a FCC lattice. A modified version of the method of reduced coordinates was used. It is important to note that in this case there is no need to resort to some approximate model or other. As a rule, the reducing parameters used are the values of $T_{mol}=\varepsilon\sqrt{k}$, $W_{mol}=\sigma^2/k\sqrt{(m/\varepsilon)}$, and $V_{mol}=N\sigma^3$, were ε and σ are the parameters of the Lennard-Jones potential, m is molecular weight and k is the Boltzmann constant. It is reasonable to use as an alternative to this the values of the temperature and molar volume of abovementioned substances at the critical points T_{cr} and V_{cr}. The choice of the given parameters is explained as follows. For simple molecular substances T_{cr} and V_{cr} are proportional to ε and σ^3, respectively. However, the accuracy of determination is much higher for the critical parameters than for the parameters of the binomial potential. It should be mentioned that the quantities ε and σ depend substantially on the choice of binomial potential and the method used to determine it. Temperature dependence of isochoric thermal resistances of Xe, CO_2 and N_2O in the reduced coordinates is shown in Fig. 4. It is seen that all the contributions to the total thermal resistance are of the same order of magnitude and the deviations from the $W\propto T$ dependence increase from Xe to N_2O. The reason has to do with increasing of the phonon scattering and approaching of Λ to its lower limit Λ_{min} as it is seen in Fig. 3.

The behavior of thermal conductivity in the orientationally-ordered phases of N_2 and CO is very similar to CO_2 and N_2O. In the orientationally-disordered β-phases isochoric thermal conductivity of all samples of different density increases with rise of temperature, whereas isobaric one is nearly temperature independent (see in Fig. 5 experimental data for N_2; data for CO is very similar). In the framework of simple kinetic model, an increase of thermal conductivity with rise of temperature may be explained by an increase of the phonon mean-free path because of the weakening of the effect of some scattering mechanism. It is logically

to assume that the interaction of phonons with rotational excitations provides such a mechanism. At the $\alpha \rightarrow \beta$ transition and over the orientationally-disordered β-phase a gradual transition from librations to hindered rotation takes place. In contrast to libration, free molecule rotation does not lead to phonon scattering. From the above it follows that there is a temperature interval where phonon scattering by the rotational excitations weakens with rise of temperature or, in other words, TO coupling decreases. The isobaric thermal conductivity is determined by partial compensation of this effect as a result of decreasing of thermal conductivity with rise of temperature due to thermal expansion.
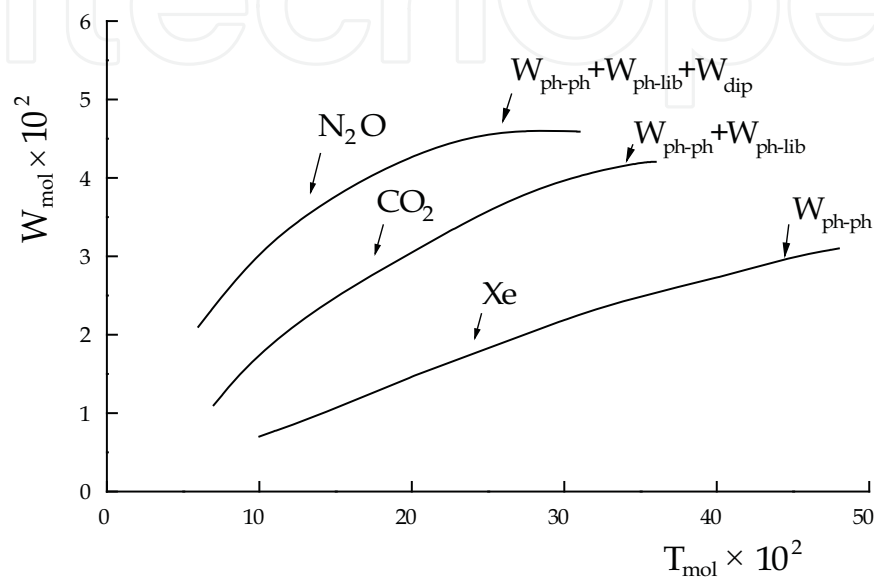

Fig. 4. Temperature dependences of isochoric thermal resistance of *Xe, CO₂* and *N₂O* in the reduced coordinates.
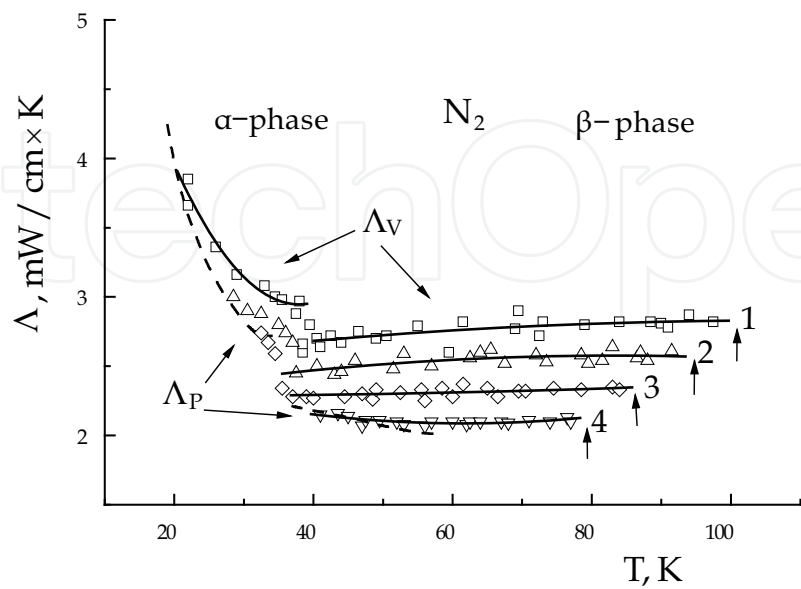

Fig. 5. Thermal conductivity of solid nitrogen. Solid lines are isochoric data for samples of different densities numbered from 1 to 4. Dashed lines are isobaric data.

Solid oxygen belongs to a small group of molecular crystals consisting of linear molecules. In contrast to the N_2-class crystals having the orientationally ordered *Pa3*-type structure, solid oxygen, much like halogens, has a collinear orientational packing because the valence rather than quadrupole forces predominate in the anisotropic interaction. Besides, in the ground state the O_2 molecule has the electron spin $S=1$ which determines the magnetic properties of oxygen. Another specific feature of solid O_2 is the fact that the energy of the magnetic interaction makes up a considerable portion of the total binding energy. This unique combination of molecular parameters has stimulated much interest in the physical properties of O_2, in particular its thermal conductivity. The thermal conductivity of solid O_2 was investigated under saturated vapor pressure in α, β and γ-phases over a temperature interval 1-52*K* (Ježowski, et al., 1993). The low-temperature α-O_2 phase is orientationally and magnetically ordered. On heating to 23.9*K*, the structure changes into the rhombohedral magnetically-ordered β-phase of the symmetry *R3m*. This is the simplest orientational structure, similar to α-O_2. On a further heating, orientational disordering (cubic cell, *Pm3m* symmetry with $Z=8$) occurs at $T=$ 43.8*K*. Under atmospheric pressure oxygen melts at 54.4*K*. The thermal conductivity has a maximum in the α-phase at $T\approx6K$, drops sharply on a change to the β-phase, where it is practically constant, jumps again at the $\beta\rightarrow\gamma$ transition and increases in γ-O_2. The experimental results were interpreted as follows. In the magnetically ordered α-phase the heat is transferred by both phonons and magnons, and their contributions are close in magnitude: $\Lambda_{ph}\approx\Lambda_m$. On the $\alpha\rightarrow\beta$ transition the thermal conductivity decreases sharply *(~60%)* because the magnon component disappears during magnetic disordering. The weak temperature dependence of the thermal conductivity in the β-phase was attributed to the anomalous temperature dependence of the sound velocity in β-O_2 which is practically constant for the longitudinal modes and increases for the transverse ones. The growth of the thermal conductivity in γ-O_2 was attributed to the decay of the phonon scattering at the rotational excitations of the molecules and at the short-range magnetic order fluctuations at rising temperature. The isochoric thermal conductivity of γ-O_2 has been studied on samples of different density in the temperature interval from 44*K* to the onset of melting (Konstantinov et al., 1998b). More sharp increase of isochoric thermal conductivity was observed in γ-O_2 than in the isobaric case.

2.3 Methane and halogenated methanes

The solid halogenated methanes consisting of tetrahedral molecules are convenient objects to investigate the correlation between the rotational motion of molecules and the behavior of thermal conductivity. Methane (CH_4), and carbon tetrahalogenides (CF_4, CCl_4, CBr_4 and CJ_4) form high-temperature "plastic" or orientationally-disordered phases in which the rotational motion of molecules is similar to their motion in the liquid state. In crystals consisting of low-symmetry molecules such as chloroform ($CHCl_3$), methylene chloride (CH_2Cl_2) or dichlorodifluoromethane (CCl_2F_2) the anisotropic forces are much stronger and the long-range order persists in them up to the melting points. A special case is trifluoromethane CHF_3, where the second *NMR* momentum decreases sharply above $T=80K$ from 11.5G^2 to 3.0G^2 immediately prior to melting at $T_m=118K$, which suggests enhancement of the molecule rotation about the three-fold axes.

The molecule of methane can be presented as a regular tetrahedron with hydrogen atoms at the vertex positions and carbon atom in the center. The symmetry causes the molecule to exhibit permanent octupole electrostatic moment. At the equilibrium vapor pressure CH_4

solidifies at 90.7*K* and displays unchanged crystallographic structure called phase *I* down to 20.4*K* which is the temperature of phase transition to phase *II*. In both phases, the carbon atoms at the center of the tetrahedral molecule occupy sites of the face-centered cubic lattice. In the low-temperature phase *II* the orientation dependent octupole-octupole interaction leads to a partial orientational ordering. The crystal structure with six orientationally-ordered and two disordered sublattices belongs to the space group *Fm3c*. The orientationally-ordered molecules at D_{2d} site symmetry positions perform collective librations, while those at O_h positions rotate almost freely down to the lowest temperatures. In phase *I* all the tetrahedral molecules are orientationally-disordered, performing rotations which do not show any long-range correlation. *CH₄(I)* is unique between ODIC molecular crystals since its molecular rotation is virtually free at premelting temperatures. The isobaric thermal conductivity of solid methane was measured within the temperature range of 21-90*K* in phase *I* (Manzhelii & Krupski, 1968) and within the temperature interval of 1.2–25*K* in phase *II* (Jeżowski et al., 1997). The results obtained revealed an existence of the strong phonon scattering mechanisms connected with rotational excitation of the methane molecules. The isochoric thermal conductivity was studied by (Konstantinov et al., 1999) on samples with molar volumes 30.5 and 31.1 *cm³/mole*. The experimental data for the orientationally-disordered phase of *CH₄(I)* is shown in Fig. 6.
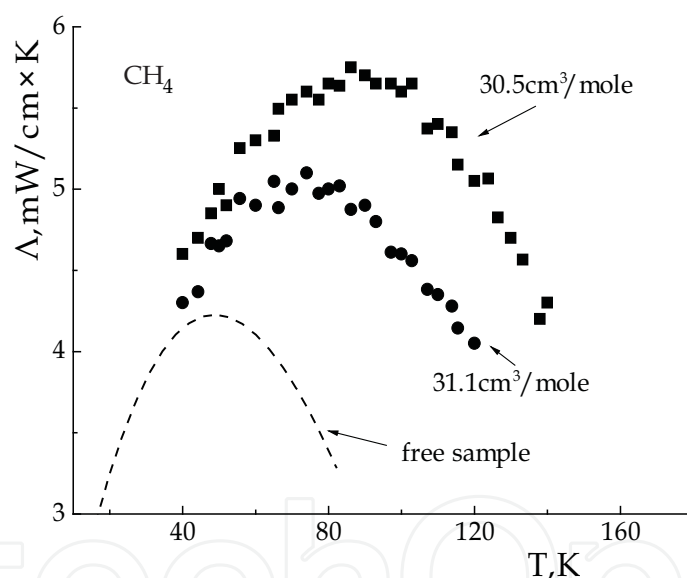

Fig. 6. The isochoric thermal conductivity of solid methane for samples having molar volumes 30.5 (■) and 31.1 (●) *cm³/mole* together with the isobaric data (dashed line).

It is seen that both isobaric and isochoric thermal conductivities first increase with rise of temperature, pass through a maximum and then decrease up to melting. Note, than regular „kinetic" maximum of thermal conductivity is observed at considerably lower temperature in phase *II* (Jeżowski et al., 1997). Maximum shifts towards higher temperatures as the density of the sample increases. The Bridgman coefficient is equal to 8.8±0.4.

The origin of such behavior of thermal conductivity is the same that for orientationally-disordered phases of other molecular crystals, it is decrease of phonon scattering on rotational excitations of molecules. However, in contrast to "plastic" phases of other molecular crystals where rotation is hindered, methane molecules rotate almost freely at premelting temperatures. Above the maximum, phonon-rotation contribution $W_{ph\text{-}rot}$ to the

total thermal resistance W of methane tend to zero, and behavior of thermal conductivity is determined solely by increase of phonon-phonon scattering. It is clearly seen in Fig. 7, where the appropriate contributions were calculated using the method of reduced coordinates. The theoretical models proposed to describe thermal conductivity of solid methane will be discussed later.
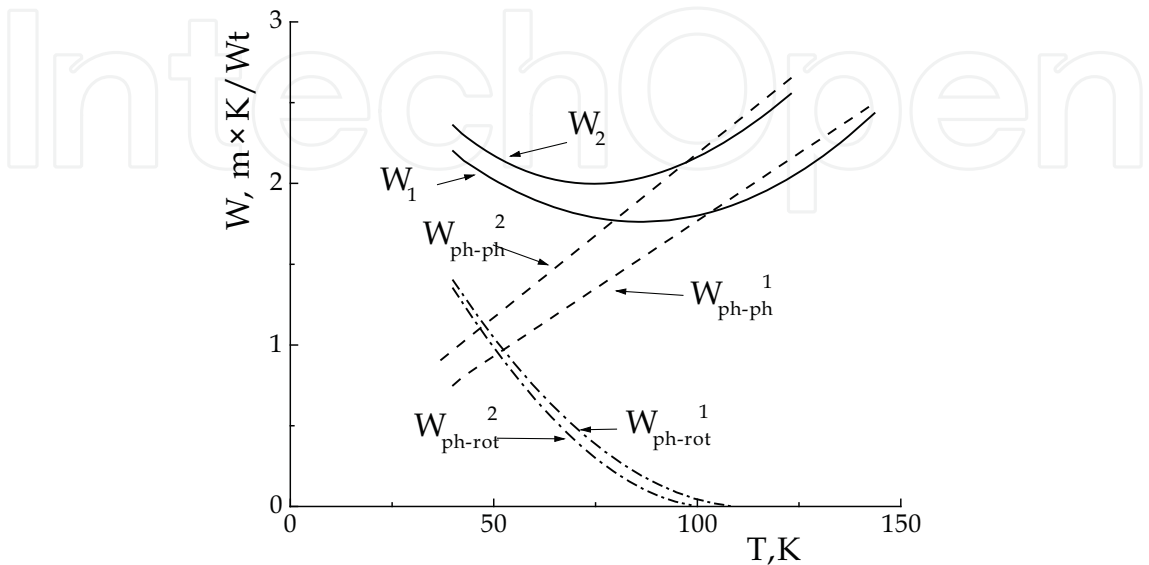

Fig. 7. Contributions of phonon-phonon scattering $W_{ph\text{-}ph}$ and phonon scattering by rotational molecule excitations $W_{ph\text{-}rot}$ to the total thermal resistance W of solid methane samples having molar volumes 30.5 (1) and 31.1 (2) $cm^3/mole$.
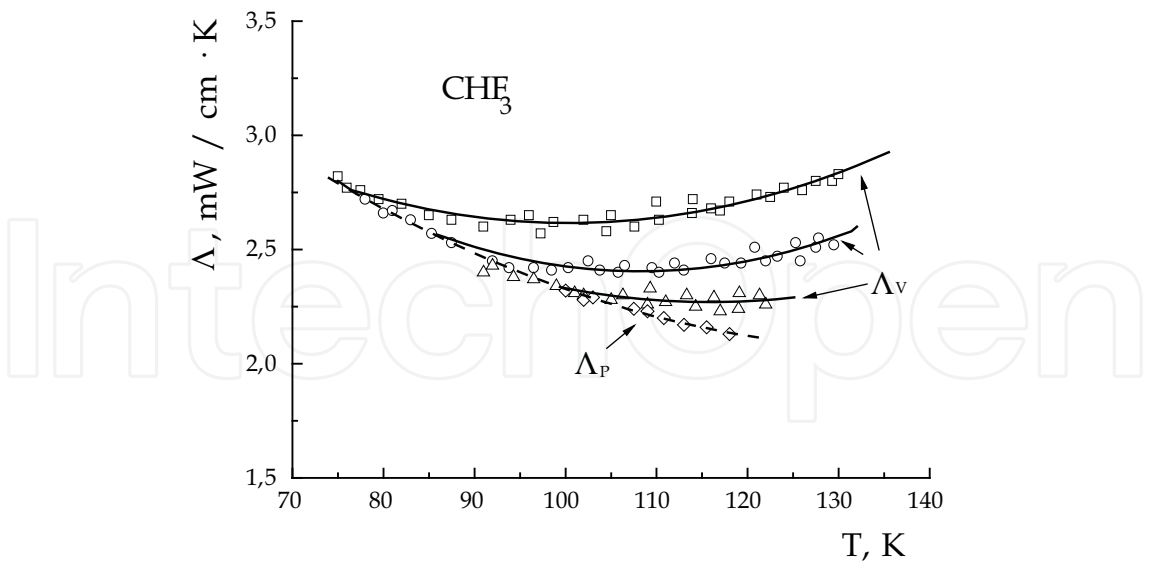

Fig. 8. The isochoric thermal conductivity of three solid CHF_3 samples of different densities. Solid lines show smoothed values of isochoric thermal conductivity. Dashed line and rhombus are for the thermal conductivity of a free sample.

Slow increase of isochoric thermal conductivity was also observed in the orientationally-disordered phases of CCl_4 (Konstantinov et al., 1991a) and CBr_4 (Ross et al., 1984) at

recalculation the last experimental data to constant volume. The isochoric thermal conductivity in orientationally-ordered phases of halogenated methanes ($CHCl_3$, CH_2Cl_2 and CCl_2F_2) decreases with rise of temperature deviating markedly from $1/T$ dependence like case of CO_2 and N_2O (Konstantinov et al., 1991b; 1994; 1995). An interesting behavior of the isochoric thermal conductivity was found in trifluoromethane CHF_3 (Konstantinov et al., 2009a). CHF_3 melts at T_m=118K, the melting entropy being $\Delta S_f/R$ = 4.14. Neutron scattering investigations of the crystallographic structure of CHF_3 revealed only one crystalline phase of the spatial symmetry $P2_1/c$ with four differently oriented molecules in the monoclinic cell. The Debye temperature of CHF_3 is Θ_D=88±5K. Fig. 8 shows isochoric thermal conductivity of CHF_3 for three samples of different densities in the interval from 75K to the onset of melting. The isochoric thermal conductivity first decreases with increasing temperature, passes through a minimum at T~100K, and then starts to increase slowly. The weak growth of isochoric thermal conductivity with temperature in solid CHF_3 suggests that the translational-orientational coupling becomes weaker in this crystal at premelting temperatures owing to the intensive molecule reorientations about the three-fold axes.

Some parameters of the halogenated methanes discussed are presented in Table 1.

Substance		T_m, T_{I-II}	Structure	z	$\Delta S_f/R$	Θ_D, K	g	μ, D
CH_4	(I)	90.6	F_m3m	4	1.24	96	8.8	0
	(II)	20.5	$P43m$	32		141		
CCl_4	(I)	250.3	F_m3m	4	1.21		6.0	0
	(II)	225.5	$C2/c$	32		92	6.5	
CBr_4	(I)	363	F_m3m	4	1.3	62	3.8	0
	(II)	320	$C2/c$	32			3.4	
CHF_2Cl	(I)	115.7	$P4_2/n$	8	4.25		4.5	1.41
	(II)	59	$P112/n$	8		70		
$CHCl_3$		210	$Pnma$	4	5.4	86*	3.9	1.01
CH_2Cl_2		176	$Pbcn$	4	3.13	115*	4.6	1.6
CF_2Cl_2		115	$Fdd2$	8	4.2	80*	5.0	0.51
CHF_3		118	$P2_1/c$	4	4.14	88*	4.6	1.6

* - Estimates obtained from *IR* and Raman spectra.

Table 1. Melting temperature T_m; phase transition temperature T_{I-II}; structure and the number of molecules per unit cell z; melting entropy $\Delta S_f/R$; Debye temperature Θ_D; Bridgman coefficient $g = -(\partial \ln \Lambda / \partial \ln V)_T$; dipole momentum of molecule μ.

2.4 Some special cases: SF_6 and C_6H_6

Sulphur haxafluoride SF_6 is often assigned to substances that have a plastic crystalline phase. Indeed, the relative entropy of melting $\Delta S_f/R$ of SF_6 is 2.61, which is close to the Timmermanns criterion. However, the nature of orientational disorder in the high-temperature phase of SF_6 is somewhat different from that of plastic phases in other molecular crystals, where the symmetries of the molecule and its surroundings do not coincide. The interaction between the nearest neighbors in the *bcc* phase is favorable for molecule ordering caused by the *S-F* bonds along the *{100}* direction, and the interaction with the next nearest neighbors is dominated by repulsion between the *F* atoms. According to *X*-ray and neutron diffraction data a strict order is observed in SF_6 *(I)* just above the phase

transition point. The structural dynamical factor $\mathcal{R}$ characterizing the degree of the orientational order is close to unity in the interval 95-130K. This feature sets off SF_6 from other plastic crystals, such as methane, carbon tetrachloride, adamantane and so on, where the long-range orientational order becomes disturbed immediately after the phase transition. Orientational disordering in SF_6 starts to intensify only above 140K. As follows from the analysis of the terms of the Debye-Waller factor derived from neutron-diffractometric data for the high-temperature phase of SF_6, the F atoms have large effective libration amplitudes. As the temperature rises, the amplitudes increase to 20° and higher, but the F localization is still appreciable near {100} direction. This implies that the orientational structure of SF_6 (I) does not become completely disordered even at rather high temperatures. The disordering itself is dynamic by nature. The increasing amplitudes of librations are not the only factor responsible for the increasing orientational disordering at rising temperature. It is rather connected with dynamic reorientations, which become more intensive due to frustrations of the molecular interactions. Owing to these features, SF_6 offers a considerable possibility for investigating the influence of wide-range rotational states of the molecules on the thermal conductivity in a monophase one-component system, where such states can vary from nearly complete orientational ordering to frozen rotation.
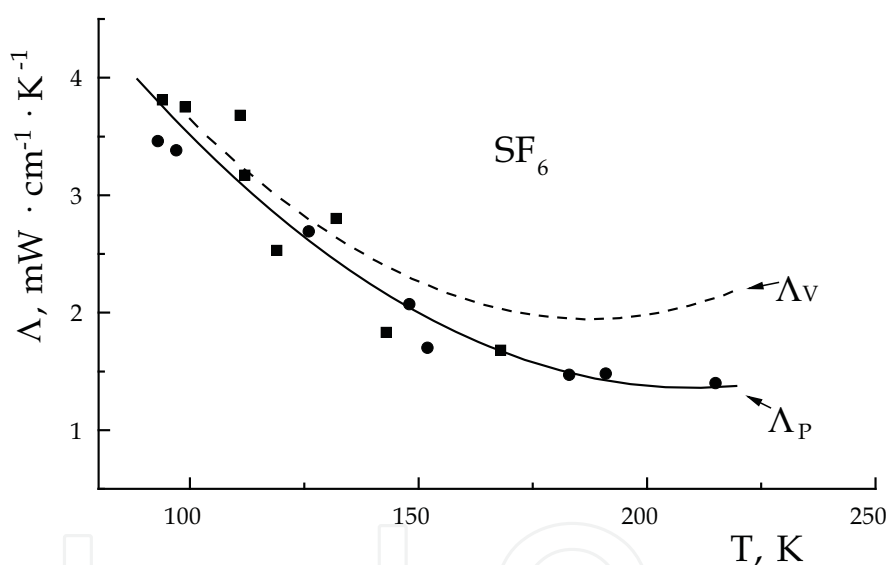

Fig. 9. Isochoric (V_m=58.25 $cm^3/mole$) and isobaric thermal conductivity of solid SF_6.

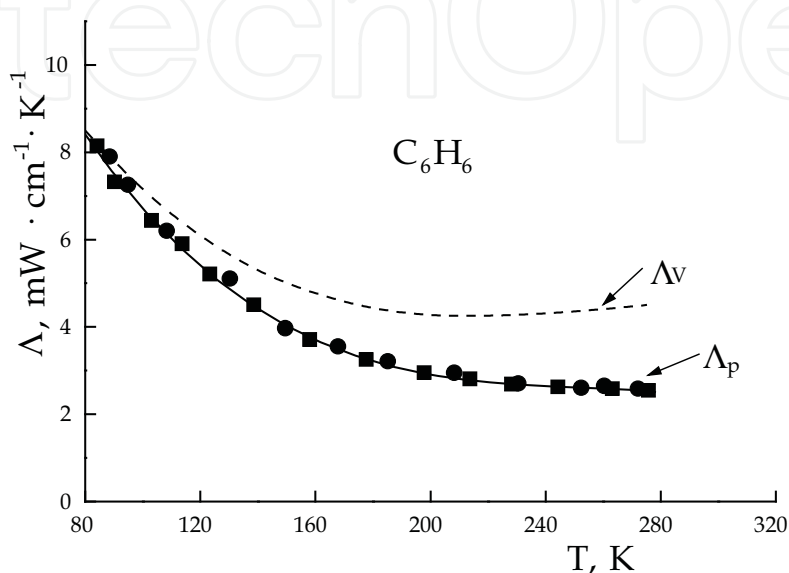Isochoric thermal conductivity of SF_6 was studied by Konstantinov et al., 1992b, while isobaric one by Purski et al., 2003. The data are shown in Fig. 9. The isobaric thermal conductivity first decreases with increasing temperature and flattens out at premelting temperatures. The isochoric thermal conductivity first decreases with increasing temperature, passes through a minimum at $T\sim180K$, and then starts to increase. Such behavior was attributed to decreasing of phonon scattering on rotational excitations of molecules with rise of temperature.

Solid benzene has only one crystallographic modification under the saturated vapor pressure: it has the orthorhombic spatial symmetry $\boldsymbol{P}bca$ (D_{2h}^{15}) with four molecules per unit cell. Benzene melts at 278.5K with entropy of melting $\Delta S_f/R$ = 4.22, which is much higher that the Timmermanns criterion for *ODIC* phases. The Debye temperature of C_6H_6 is 120K. In the interval 90-120K the second *NMR* moment of C_6H_6 drops considerably as a result of

the molecule reorientations in the plane of the ring around the six-fold axis. The activation energy of the reorientational motion estimated from the spin-lattice relaxation time is 0.88 *kJ/mole*. The frequency of molecule reorientations at 85*K* is 10^4 *sec^{-1}*. On a further heating it increases considerably reaching 10^{11} *sec^{-1}* near T_m. The basic frequency of the benzene molecule oscillations about the six-fold axis at 273*K* is 1.05×10^{12} *sec^{-1}*. Isochoric thermal conductivity of C_6H_6 was studied by Konstantinov et al., 1992a, while isobaric one by Purski et al., 2003. The data are shown in Fig. 10.

Fig. 10. Isochoric (V_m=70.5 *cm³/mole*) and isobaric thermal conductivity of solid C_6H_6.

Like solid SF_6 the isobaric thermal conductivity of benzene first decreases with increasing temperature and flattens out at premelting temperatures. The isochoric thermal conductivity first decreases with increasing temperature, passes through a minimum at $T \sim 210K$, and then starts to increase slowly. In contrast to SF_6 where the rotation is multi-axial, molecule of benzene rotates about released six-fold axis. The increase of thermal conductivity with rise of temperature was attributed like to previous cases to weakening of phonon scattering on rotational excitations of molecules.

2.5 Solid n-alkanes

Normal alkanes (*n*-paraffins) of the C_nH_{2n+2}-type form a class of substances that are intermediate in changing–over to long–chain polymers. *N*–alkanes have a comparatively simple structure and a molecular packing: in the solid state the axes of all molecules are always parallel to one another irrespective of a particular crystalline modification. Owing to their relative simplicity, normal alkanes are naturally considered as the starting point for understanding the structural and thermophysical properties of more complex long–chain compounds. *N*–alkanes exhibit an extremely diverse dynamic behavior both in the solid and liquid states. The melting temperature increases in this series of compounds with the length of the chain and its behavior is nonmonotonic: the *n*–alkanes with an odd number of carbon atoms (odd *n*–alkanes) melt at relatively lower temperatures than those with an even number of *C* atoms (even *n*–alkanes). An interesting effect is observed when the orthorhombic, monoclinic and triclinic structures alternate with the even and odd

members of the series. The even *n*–alkanes with *n*=6–24 (*n*=the number of *C* atoms) crystallize at low temperatures forming a triclinic cell. Heptane (*n*=7) and nonane (*n*=9) have an orthorhombic structure at low temperatures. Glass–like cylindrical "rotational" phases with a hexagonal symmetry were found in rather narrow temperature interval below the melting points of odd *n*–alkanes starting with *n*=9. The region of existence of the "rotational" phase increases with the length of the chain. Hexagonal modifications also occur in even *n*–alkanes starting with *n*=22. Some parameters of *n*-alkanes discussed above are submitted in Table 2.

Substance	structure	$T_{\alpha-\beta}$,K	$\Delta S_{\alpha-\beta}/R$	T_m,K	$\Delta S_m/R$	$\Delta S_{\alpha-L}/R$	Λ_α/Λ_L
C_2H_6	$P2_1/n$, z=2	89.8	2.74	90.3	0.77	3.6	1.3
C_3H_8	$P2_1/n$, z=4	-	-	85.5	4.95	4.95	2.2
C_6H_{14}	P ī, z=1	-	-	177.8	8.85	8.85	1.9
C_9H_{20}	P ī, z=1	217.2	3.48	219.7	8.47	12.0	2.4
$C_{11}H_{24}$	P_{bcn}, z=4	236.6	2.9	247.6	10.8	13.7	2.4
$C_{13}H_{28}$	P_{bcn}, z=4	255.0	3.6	267.8	12.8	16.4	2.3
$C_{15}H_{32}$	P_{bcn}, z=4	270.9	4.1	283.1	14.7	18.8	2.1
$C_{17}H_{36}$	P_{bcn}, z=4	284.3	4.8	295.1	16.4	21.2	2.0
$C_{19}H_{40}$	P_{bcn}, z=4	296.0	5.6	304.0	18.8	24.3	2.0

Table 2. The structure of *n*-alkanes; the temperature $T_{\alpha\beta}$ and the entropy $\Delta S_{\alpha\beta}/R$ of the transition to the "rotational" phase; the temperature T_m and the melting entropy $\Delta S_m/R$; a complete change of the entropy and variations of thermal conductivity Λ_α/Λ_L during the ordered-phase – liquid transition.

The isochoric thermal conductivity of methane, ethane, propane and hexane was studied by Konstantinov et. al., 1999a; 2006c; 2009b and 2010 correspondingly. Isobaric thermal conductivity of "odd" numbered *n*-alkanes with *n=9-19* was investigated by Forshman & Andersson, 1984. The isobaric thermal conductivity of n-alkanes discussed above is shown in Fig. 11 along with the thermal conductivities of the liquid phases of these compounds measured immediately after melting. It was noted (Forshman & Andersson, 1984) that the thermal conductivity of long–chain odd *n*-alkanes has some features in common. As the "rotational" phase melts, the thermal conductivity changes by about 35% and is independent of the chain length. The jump of the thermal conductivity on changing to the low temperature ordered phase decreases with the increasing length of the chain and makes ~85% for *n*-undecane and ~40% for *n*-nonadecane. The absolute value of thermal conductivity increases in the "rotational" phase with increasing of the chain length.

According to our studies the isobaric thermal conductivity exhibits closely similar behavior in short and long–chain *n*-alkanes. On the transition from the ordered phase to a liquid the thermal conductivity of the *n*-alkanes starting with propane changes nearly twice and is independent of the total transitions entropy and the chain length. This change is much smaller in the case of spherical and elliptic molecules: for example, $\Delta\Lambda/\Lambda_L$ is only 20–30% in methane and ethane. This can be related to the higher degree of orientational order in solid long–chain *n*-alkanes as compared to spherical molecules. The isochoric thermal conductivity of solid *n*-alkanes decreases with rise of temperature following a dependences

weaker than $\Lambda \propto 1/T$. The deviation of the isochoric thermal conductivity from the dependence $\Lambda \propto 1/T$ in solid *n*-alkanes was explained proceeding from the concept of the lower limit to thermal conductivity (Konstantinov et. al., 2009b).
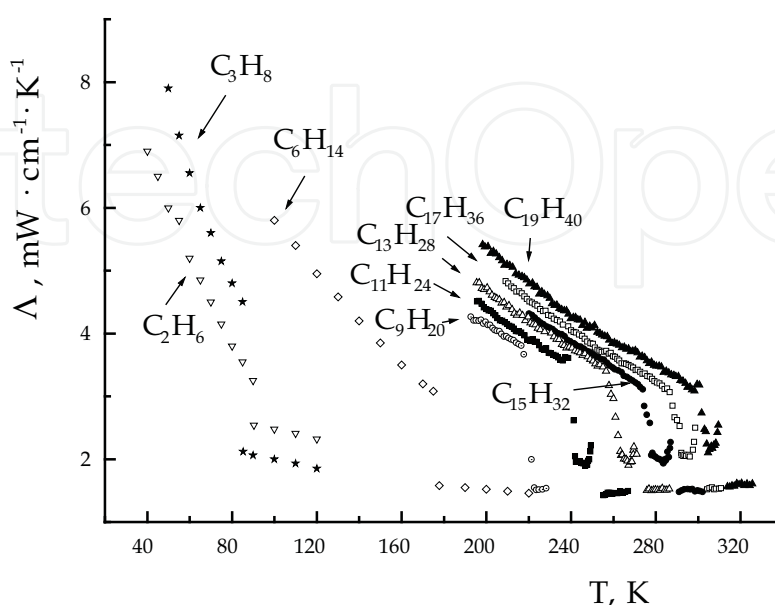

Fig. 11. Isobaric thermal conductivity of some *n*-alkanes.

2.6 Mixed molecular crystals

Mixed molecular crystals are convenient object for testing of the concept of the lower limit to thermal conductivity. In heavy solidified inert gases *Ar*, *Kr* and *Xe* the thermal conductivity approaches its lower limit at premelting temperatures. In the case when the thermal conductivity approaches Λ_{min} with rise of temperature, the effect of impurities should manifest itself in a specific manner. Impurities cannot considerably decrease the thermal conductivity at premelting temperatures at which Λ has already been close to the minimum value. As temperature decreases the contribution of impurities to the thermal resistance of crystal $W=1/\Lambda$ should increase. The isochoric thermal conductivity of solid $(CH_4)_{1-\xi}Kr_\xi$, $Kr_{1-\xi}Xe_\xi$ and $(CO_2)_{1-\xi}Kr_\xi$, $(CO_2)_{1-\xi}Xe_\xi$ solutions $(\xi=0\div1)$ has been studied by Konstantinov et al., 2000, 2001a; 2002b and 2006b, respectively. Fig. 12 shows the temperature dependence of isochoric thermal conductivity for pure *Kr* and $Kr_{1-\xi}Xe_\xi$ solid solution reduced to samples for which condition of constant volume starts from 80K.

It can be seen that the thermal conductivity of $Kr_{1-\xi}Xe_\xi$ solid solution decreases and its temperature dependence becomes weaker with an increase in *Xe* concentration. At $\xi=0.14$, the thermal conductivity virtually coincides with the lower limit to thermal conductivity calculated by Eq. 4.

Kr and *CH₄* form a homogeneous solid solution with **fcc** structure above 30K at all ξ. They have similar molecule/atom radii and parameters of the pair potential. The Debye temperatures Θ_D of *Kr* and *CH₄* are 72 and 143K respectively. At the same time the masses of the *Kr* atom and the *CH₄* molecule are very different, 83.8 and 16 atomic units, respectively. The isochoric thermal conductivity of $(CH_4)_{1-\xi}Kr_\xi$ solid solutions has been studied between 40K and ~ 150K over the wide range of concentrations, (ξ=0.013, 0.032, 0.07, 0.115, 0.34, 0.71,

0.855, 0.937, and 0.97). A gradual transition from the thermal conductivity of a highly perfect crystal to the minimum thermal conductivity was observed as the crystal becomes increasingly more disordered (see Fig. 13).
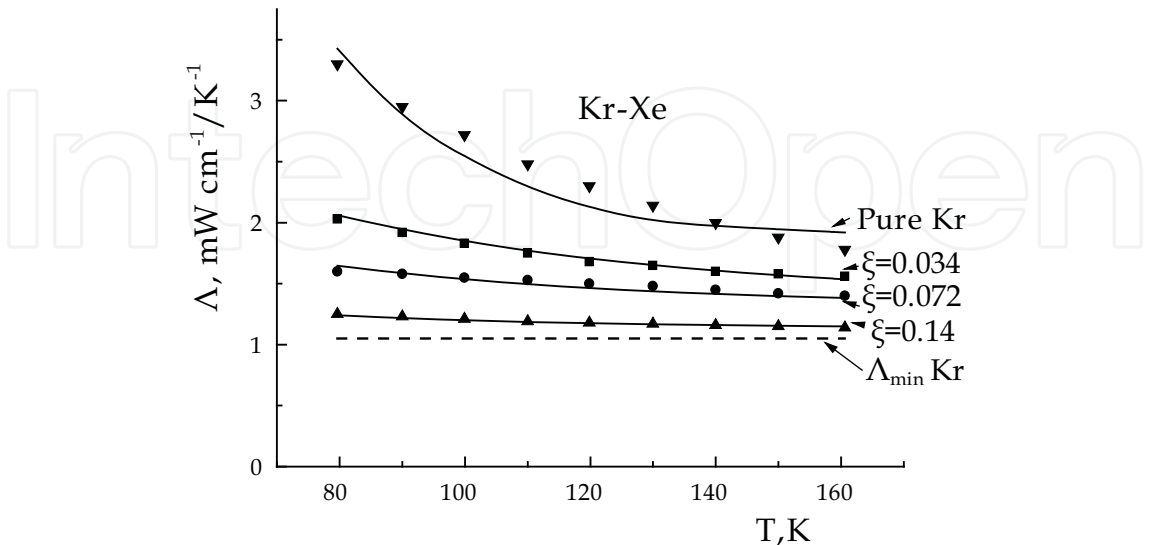

Fig. 12. Smoothed values of isochoric thermal conductivity of pure Kr and $Kr_{1-\xi}Xe_{\xi}$ solid solution for samples, whose volume is constant starting from $80K$. The dashed line is Λ_{min} of pure Kr, calculated according to Eq. 4.
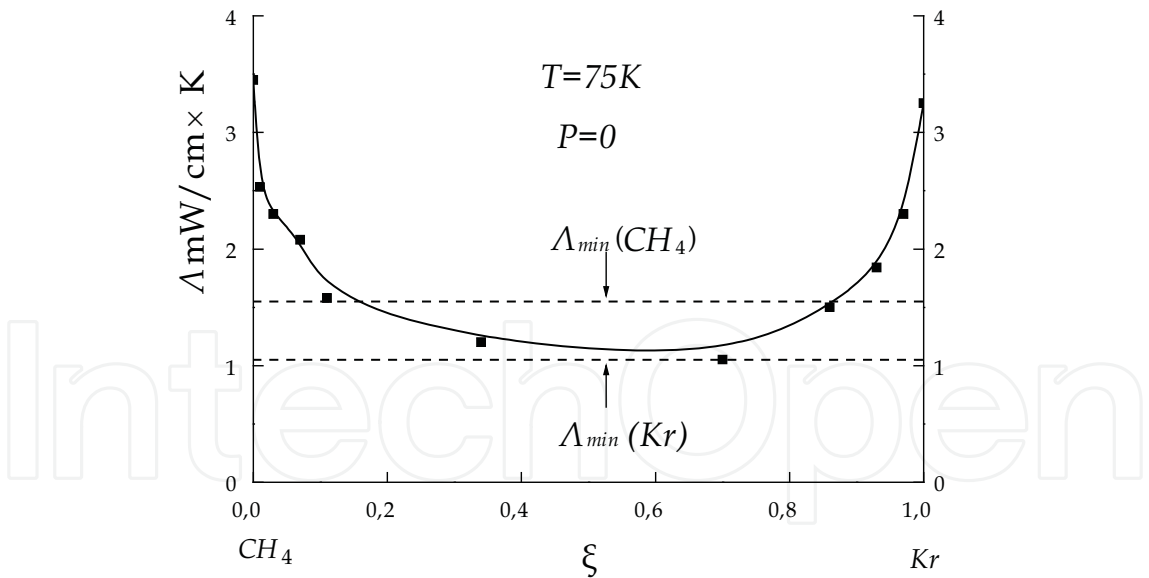

Fig. 13. The concentration dependence of the thermal conductivity of solid solution $(CH_4)_{1-\xi}Kr_{\xi}$ at $T=75K$ and $P=0$. The horizontal lines are Λ_{min} of pure Kr and CH_4 under the same conditions calculated by Eq. 4.

A strong decrease of the Bridgman coefficient was observed, from a value $g\cong9$ characteristic for pure Kr and CH_4 to $g\cong4$ at only a tiny impurity concentration.
An unusual effect of point defects on the thermal conductivity has been detected in $(CO_2)_{1-\xi}Xe_{\xi}$ and $(CO_2)_{1-\xi}Kr_{\xi}$ solid solutions (Konstantinov et al., 2006b). In pure CO_2 at $T>150K$ the

isochoric thermal conductivity decreases smoothly with increasing temperature. In contrast, the thermal conductivity of CO_2 /Kr and CO_2 /Xe solid solutions first decreases, passing through a minimum at 200–210K, and then starts to increase with temperature up to the onset of melting. Such behavior of the isochoric thermal conductivity was attributed to the rotation of the CO_2 molecules, which gain more freedom as the spherically symmetrical inert gas atoms are dissolved in the CO_2.

2.7 Short conclusion to the experimental part

It has been demonstrated that the $\Lambda \propto 1/T$ law is not obeyed in molecular crystals at all. Because of the strong translational-orientational (TO) coupling in the orientationally-ordered phases molecular librations contribute considerably to the thermal resistance $W=1/\Lambda$ of the crystal. As a result, the isochoric thermal conductivity approaches its lower limit Λ_{min} at premelting temperatures and shows significantly more slow dependence than $1/T$. In the case of hindered or almost free rotation of molecules in crystal the isochoric thermal conductivity increases with rise of temperature. It is originated due to weakening of TO coupling as the rotational motion of molecules attains more freedom. The isobaric thermal conductivity is determined by the partial compensation of these effects as a result of decreasing of thermal conductivity with rise of temperature due to thermal expansion.

3. Theoretical models.

3.1 The Debye model of thermal conductivity

In simple Debye model (see, for example, Berman, 1976) thermal conductivity Λ can be expressed as

$$\Lambda = \frac{\hbar^2}{2\pi^2 \mathrm{v}^2 k_B T^2} \int\limits_0^{\omega_D} l_\Sigma(\omega)\omega^4 \frac{e^{\frac{\hbar\omega}{k_B T}}}{\left(e^{\frac{\hbar\omega}{k_B T}} - 1\right)^2} d\omega, \tag{7}$$

where v is the sound velocity; ω_D is the Debye frequency $\omega_D = v(6\pi^2 n)^{1/3}$; $l_\Sigma(\omega)$ is the combined phonon mean-free path determined by the package of all scattering mechanisms

$$l_\Sigma(\omega) = \left(\sum_i l_i(\omega)^{-1}\right)^{-1}, \tag{8}$$

If the scattering governed by U-processes only the mean-free path of phonons is

$$l_u(\omega) = \mathrm{v}\big/ A\omega^2 T, \quad A = \frac{18\pi^3}{\sqrt{2}}\frac{k_B \gamma^2}{ma^2 \omega_D^3}; \tag{9}$$

were m is the average atomic (molecular) mass; a^3 is the volume per atom (molecule); $\gamma = -(\partial \ln \Theta_D/\partial \ln V)_T$ is the Grüneisen parameter. It is easy to check that in high-temperature limit $T \geq \Theta_D$ Eqs. 7 and 9 reduce to Eq. 1. In the case of point defect scattering the mean-free path of phonons is

$$l_i(\omega) = v / B\omega^4 \; ; \; B = \frac{3\pi\Gamma}{2\omega_D^3} \; ; \; \Gamma = \xi(1-\xi)\left(\frac{\Delta M}{\overline{M}} + 6\gamma\frac{\Delta a}{\overline{a}}\right)^2 \tag{10}$$

where ΔM is the mass difference of atoms (molecules) of the impurity and host; Δa is the change of the lattice parameter upon introduction of impurity.

3.2 Phonon-libron scattering

The contribution of phonon-libron scattering was considered by (Manzhelii et al., 1975), and (Kokshenev et al., 1997). In harmonic approximation decomposition of the interaction energy with respect to translational and angular displacements of molecules near equilibrium positions can be written as

$$H_{harm} = \sum_{\vec{q},\lambda} \hbar\omega_{\vec{q},\lambda}\left(b^+_{\vec{q},\lambda}b_{\vec{q},\lambda} + \frac{1}{2}\right) + \sum_{\vec{k},j} \varepsilon_j\left(a^+_{\vec{k},j}a_{\vec{k},j} + \frac{1}{2}\right), \tag{11}$$

where $b_{\vec{q},\lambda}$, $a_{\vec{k},j}$ are the operators of deletion of phonons and librons; λ and j are the numbers of phonon and libron branches. So long as the anharmonicity of molecular librations is substantial even at low temperatures a self-consistent theory was used for description of the libron subsystem (see, for example, Manzhelii et al., 1997). Only the interaction processes leading to the linear dependence of thermal resistance in high temperature $T \geq \Theta_D$ limit were taken into consideration

$$V = \frac{\gamma_1 aG}{\sqrt{N}} \sum_{q,q',k} \sqrt{qq'} a^+_k b_q b_{q'} \Delta(k-q-q') + \gamma_2 G\sqrt{a/N} \sum_{q,k,k'} \sqrt{q} a_k a^+_{k'} b_a \Delta(k-k'+q), \tag{12}$$

where $k \equiv (\vec{k},j)$, $q \equiv (\vec{q},\lambda)$; N is number of lattice points; $G = U\eta$ (U is a constant of molecular field, η is a parameter of the long-range orientational order). In Eq. 12 only the members were taken into consideration which allow for conservation law of energy and quasi-momentum. Three types of interactions were considered:

$$Ph_A + Ph_A \leftrightarrow Lib, \tag{13a}$$

$$Ph_A + (Ph_O \; or \; Lib) \leftrightarrow (Lib \; or \; Ph_O), \tag{13b}$$

$$Ph_A + Lib \leftrightarrow Lib', \tag{13c}$$

where Ph_A and Ph_O designate acoustic and optical phonons. The constants of interactions γ_1 and γ_2 can be expressed via characteristic temperatures Θ and Θ_l of translational and librational spectrum of crystal:

$$\gamma_1 = C_1 \hbar^3 / Ma^2 \Theta(J\Theta_l)^{1/2} \; k_B^{3/2}, \tag{14a}$$

$$\gamma_2 = C_2 \hbar^3 / J\Theta_l (Ma^2\Theta)^{1/2} \; k_B^{3/2}, \tag{14b}$$

where J is a momentum of inertia of molecule. In quasi-harmonic approach the characteristic temperature is associated with a value of barrier G hindering of molecular rotation by the relation

$$\Theta_l = (3\hbar^2 G / J\, k_B^2)^{1/2}, \tag{15}$$

An additional thermal resistance of crystal determined by scattering processes of the type (13a) and (13b) can be presented as

$$W_1(T) = C_1 T \left(\frac{h}{k_B}\right)^3 \frac{\gamma_{lib}^2}{ma\Theta^3} \frac{ma^2}{J} S_1 \,; \qquad S_1 = \sum_\nu g_\nu \varphi_\nu \,, \tag{16a}$$

$$W_2(T) = C_2 T \left(\frac{h}{k_B}\right)^3 \frac{\gamma_{lib}^2}{ma\Theta^3} \frac{ma^2}{J} S_2 \,; \qquad S_2 = \sum_{\nu,\nu'} g_\nu g_{\nu'} f_{\nu,\nu'} \,, \tag{16b}$$

where γ_{lib} is Grüneisen parameter; g_ν and $g_{\nu'}$ are degrees of degeneration of libron and optical branches; m and J are the mass and momentum of inertia of molecule; a is inter-atomic distance; φ_ν and $f_{\nu,\nu'}$ are the surfaces of energy conservations in scattering processes like (13a) and (13b). In the simple Ziman model they can be written as:

$$\varphi_\nu = (\alpha_\nu^2 - 1)(6\alpha_\nu - 4 - \alpha_\nu^3) \,; \quad \alpha_\nu = \theta_\nu / \theta, \tag{17a}$$

$$f_{\nu,\nu'} = \sigma_{\nu,\nu'}^3 (12 - \sigma_{\nu,\nu'}^2) \,; \qquad \sigma_{\nu,\nu'} = \left| \Theta_\nu - \Theta_{\nu'} \right| / \Theta, \tag{17b}$$

where θ_ν and $\Theta_{\nu'}$ are the frequencies of optical and phonon modes.

The total thermal resistance of crystal at presence of phonon-phonon and two phonon-libron mechanisms of scattering in the reduced coordinates is:

$$W^* = B^* T^* = B_0^* T^* \left[1 + (ma^2 / J)(\alpha S_1 + \beta S_2) \right], \tag{18}$$

where coefficients B_0^*, α and β are equal for the group of one-type crystals. By this means that an additional phonon-libron scattering leads in the first approximation only to renormalization of coefficient A in Eq. 9.

3.3 Phonon scattering on rotational excitations of molecules

In the orientationally-disordered phases of molecular crystals there is no long-range order, what suggests that the distinct pure libration modes cannot propagate in the crystal. Nevertheless, the correlation effects are still strong immediately after the phase transition and the short-range orientational order persists. In this region there is an additional phonon scattering at the short-range orientational order fluctuations and it becomes weaker on a further temperature rise. To explain the behaviour of the thermal conductivity in the orientationally-disordered phases of solid methane and deuteromethane Manzhelii & Krupski, 1968 used the analogy between molecular and spin systems. In a number of magnetic crystals the thermal conductivity was observed to increase above the magnetic phase transition. Reason for these anomalies is the scattering of phonons by critical fluctuations of the short-range magnetic order above the Neel point (Kawasaki, 1963). In the orientationally-disordered phases of the molecular crystals an increase of the isochoric thermal conductivity with increasing temperature is due to weakening of phonon scattering by fluctuations of the short-range orientational order. By existing analogy, using the

equations for one and two-phonon relaxation times of Kawasaki, 1963, the phonon mean-free path of each of the examined scattering mechanisms can be expressed as

$$l_I(\omega) = \rho\upsilon^5 / B^2 \Lambda_{rot} T \omega^2, \tag{19a}$$

$$l_{II}(\omega) = \pi\rho^2\upsilon^8 / C^2 k_B C_{rot} T^2 \omega^4, \tag{19b}$$

where B and C are anisotropic molecular interaction constants; Λ_{rot} and C_{rot} are the thermal conductivity and the heat capacity of the rotational subsystem, respectively; ρ is the density. It is assumed that $B=C^2$ in the first approximation. The coefficient B can be roughly estimated from the dependence of the phase transition temperature T_f upon pressure $B = -\chi_T^{-1}\partial(\ln T_f)/\partial P$, where χ_T is isothermal compressibility. The thermal conductivity of the rotational subsystem can be calculated from the known gas-kinetic expression $\Lambda_{rot} = \frac{1}{3}C_{rot}a^2\tau^{-1}$, where τ is the characteristic time of the site-to-site transfer of the rotational energy and can be estimated as a mean period of the librations. Taking into account Eqs. (8, 9, 19a, 19b), the phonon mean-free path in the orientationally-disordered phase can be written as

$$l_\Sigma(\omega) = \left(\frac{AT\omega^2}{\upsilon} + \frac{B^2\Lambda_{rot}T\omega^2}{\rho\upsilon^5} + \frac{C^2 k_B C_{rot} T^2 \omega^4}{\pi\rho^2\upsilon^8} \right)^{-1}, \tag{20}$$

The validity of such description was corroborated subsequently by the first principles calculations of the thermal conductivity of methane by Yasuda, 1978.

3.4 Phonons and "diffusive" modes

Eq. 8 is inapplicable if $l(\omega)$ becomes of the order of or less than half the phonon wavelength $\alpha\lambda/2 = \alpha\pi\mathrm{v}/\omega$, where α is a numerical factor of the order of unity (Roufosse & Klemens, 1974).

$$l(\omega) = \begin{cases} l_\Sigma(\omega), & 0 \le \omega \le \omega_0, \\ \alpha\pi\upsilon/\omega = \alpha\lambda/2, & \omega_0 < \omega \le \omega_D, \end{cases} \tag{21}$$

Taking into account Eqs. 9, 18, and 21 the phonon mobility edge ω_0 is equal for orientationally-ordered molecular crystals to

$$\omega_0 = 1/\alpha\pi AT. \tag{22}$$

Eq. 21 is the well-known Ioffe-Regel' criterion, which presumes localization, so that we shall assume excitations whose frequencies lie above the phonon mobility edge ω_0 to be "localized". Since completely localized states do not contribute to the thermal conductivity, localization is assumed to be weak and excitations can hop from site to site in a diffusion manner, as Cahill et al., 1992 supposed. This point of view is, on the hole, consistent with the results of Feldman et al., 1993, where the theory for intermediate case (where disorder is sufficient for oscillations not to propagate but insufficient for localization) was formulated for amorphous silicon. The idea was that the dominant scattering was correctly described by

a harmonic Hamiltonian and reduced to a single-particle problem of decoupled oscillators. On this basis the thermal conductivity could be calculated exactly using a formula similar to the Kubo-Greenwood formula for the electric conductivity of disordered metals (Auerbach et al., 1984). The calculation performed by authors showed that in this case it is incorrect to indentify the Ioffe-Regel' edge with localization. Although the oscillations dominating in high-temperature heat transfer lie near the Anderson localization edge, with the exception of narrow band of states they are not completely localized. The Boltzmann theory assigns to each vibrational mode with wave vector $\vec{k}$ and propagation velocity $\vec{v} = \partial\omega / \partial\vec{k}$ a diffuseness $D_k = vl/3$, where l is the mean-free path length. The authors found that even though vibrations are not localized, a definite wave vector or velocity cannot be assigned to them. Nonetheless, they transfer heat and contribute to the thermal conductivity an amount of the order of $C_i(T)D_i/V$ for the ith mode, where the specific heat $C_i(T) = k_B$ for $T \geq \Theta_D$, D_i is the temperature-independent "diffuseness" of the mode. The numerical calculation is in many respects similar to the calculation performed according to Boltzmann's theory and it confirms the concept of a "minimum" thermal conductivity in the form it is discussed by Roufosse & Klemens, 1974; Slack, 1979 and Cahill et al., 1992.

If $\omega_0 \geq \omega_D$, then the mean-free path length of all modes is greater than $\lambda/2$ and Eqs. 7 and 22 come to Eq. 1 at $T \geq \Theta_D$. If $\omega_0 < \omega_D$, then the integral of thermal conductivity (7) splits into two parts which describe the contributions of low-frequency phonons and high-frequency "diffusive" modes to heat transfer:

$$\Lambda = \Lambda_{ph} + \Lambda_{dif} \qquad (23)$$

In the high-temperature limit $T \geq \Theta_D$ these contributions are

$$\Lambda_{ph} = \frac{k_B \omega_0}{2\pi^2 \mathrm{v}\, A T} \; ; \; \Lambda_{dif} = \frac{\alpha k_B}{4\pi \mathrm{v}}(\omega_D^2 - \omega_0^2) , \qquad (24)$$

The experimental results for a number of crystals were computer-fitted by the least-square method (see for details Konstantinov et al., 2003b). Figs. 14 and 15 show the contributions of phonons and "diffusive" modes to the isochoric thermal conductivity of Kr and CO_2.
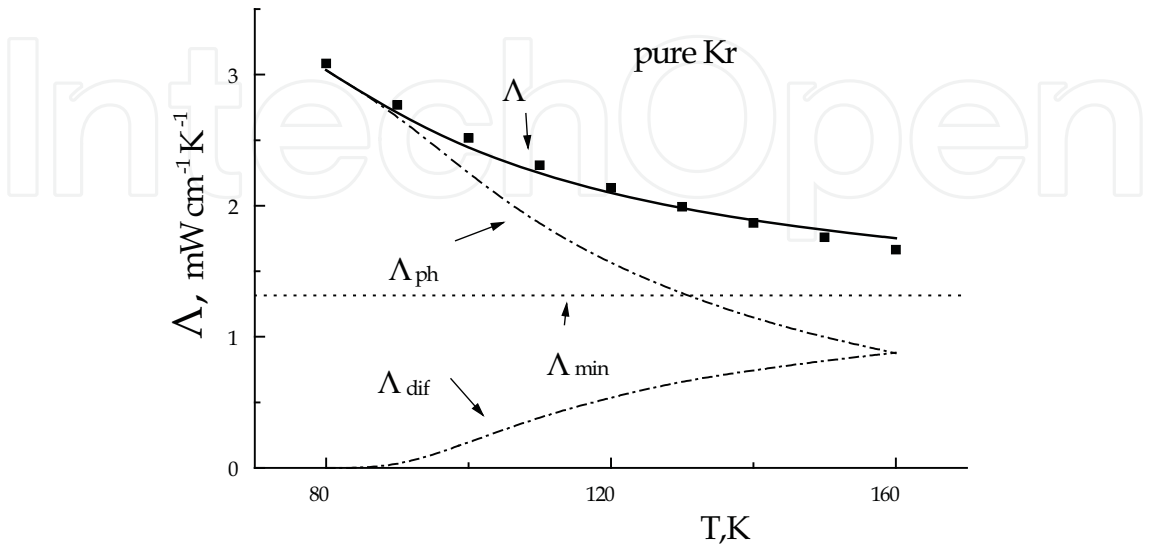

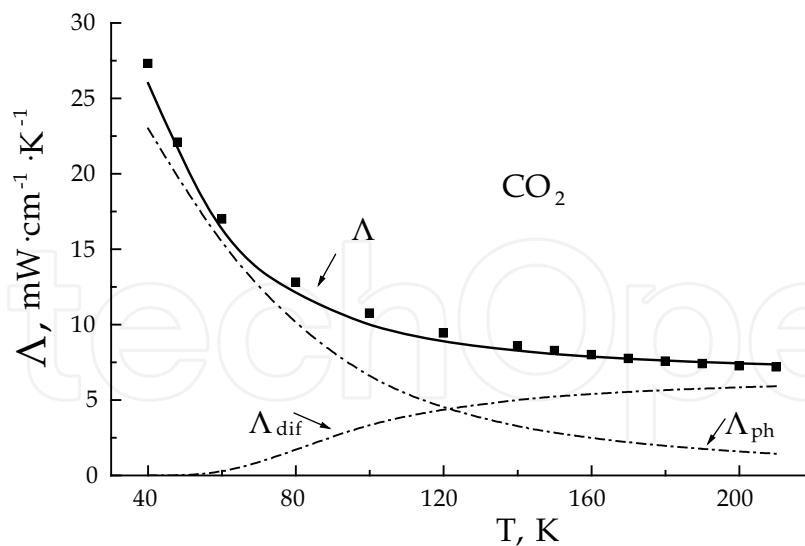Fig. 14. Contributions Λ_{ph} and Λ_{dif} for Kr sample with molar volume 28.5 $cm^3/mole$.

Fig. 15. Contributions Λ_{ph} and Λ_{dif} for CO_2 sample with molar volume 25.8 $cm^3/mole$.

It is seen that in *Kr* thermal conductivity possesses pure phonon character up to 80*K*. "Diffusive" modes arise above 80*K* and $\Lambda_{ph} \cong \Lambda_{dif}$ at 160*K*. In *CO₂* where the strong additional phonon scattering arises due to TO coupling, "diffusive" modes arise at 50*K* and in the high temperature region most part of the heat is transferred by "diffusive" modes.

The applicability of such description is supported by the straightforward calculations of the thermal conductivity by the method of molecular dynamics using the Kubo-Greenwood formula. Recently, the thermal conductivity of solid argon with the Lennard-Jones potential has been described using two contributions made by low-frequency phonons with mean-free paths exceeding half the wavelength and high-frequency phonons with mean-free path of about half the wavelength (McGaughey & Kaviany, 2004).

In the orientationally-disordered phases ω_0 follows from Eqs. (20) and (21):

$$\omega_0 = -\frac{u}{\left(-\eta + \sqrt{u^3 + \eta^2}\right)^{\frac{1}{3}}} + \left(-\eta + \sqrt{u^3 + \eta^2}\right)^{\frac{1}{3}} \tag{25}$$

where the parameters *u* and η are

$$u = \frac{\pi \rho^2 \upsilon^7}{3C^2 k_B C_{rot} T}\left(A + \frac{B^2 \Lambda_{rot}}{\rho \upsilon^4}\right), \quad \eta = -\frac{\rho^2 \upsilon^7}{2\alpha C^2 k_B C_{rot} T^2} \tag{26}$$

The appropriate contributions to the thermal conductivity from the low-frequency phonons Λ_{ph} and the high-frequency "diffusive" modes Λ_{dif} are

$$\Lambda_{ph} = \frac{\hbar^2}{2\pi^2 v^2 k_B T^2} \int_0^{\omega_0} l_\Sigma(\omega) \omega^4 \frac{e^{\frac{\hbar\omega}{k_B T}}}{\left(e^{\frac{\hbar\omega}{k_B T}} - 1\right)^2} d\omega \tag{27a}$$

$$\Lambda_{dif} = \frac{\alpha\hbar^2}{2\pi v k_B T^2} \int_{\omega_0}^{\omega_D} \omega^3 \frac{e^{\frac{\hbar\omega}{k_B T}}}{\left(e^{\frac{\hbar\omega}{k_B T}} - 1\right)^2} d\omega \qquad (27b)$$

Figs. 16 and 17 show the ratio ω_0/ω_D upon temperature and contributions Λ_{ph} and Λ_{dif} to the thermal conductivity of solid *CO*. The results were computer-fitted by the least-square method to the smoothed values of the thermal conductivity of the sample with V_m=27.93 *cm³/mole* individually in the *a*– and *β*–phases. The polarization–averaged sound velocity corresponding to this density was 1280 *m/s*. It was assumed that C_{rot} varies linearly from the value *2R* to *R* during *β*–phase (Manzhelii et al. 1997). The varied parameters were *a* and *A* in the *a*–phase and *a, A* and *B* in the *β*–phase. The best agreement with the experimental results was achieved with *a=1.55* and *A= 4.3 ×10⁻¹⁶ s/K* in the *a*–phase and with *a=1.25, A= 1.0×10⁻¹⁷ s/K, B=5.0* and *C=2.24* in the *β*–phase. As the temperature rises, the ratio ω_0/ω_D decreases in the *α*-phase and increases in the *β*-phase. This increase can be attributed to decreasing of rotational correlations between the neighboring molecules become weaker.
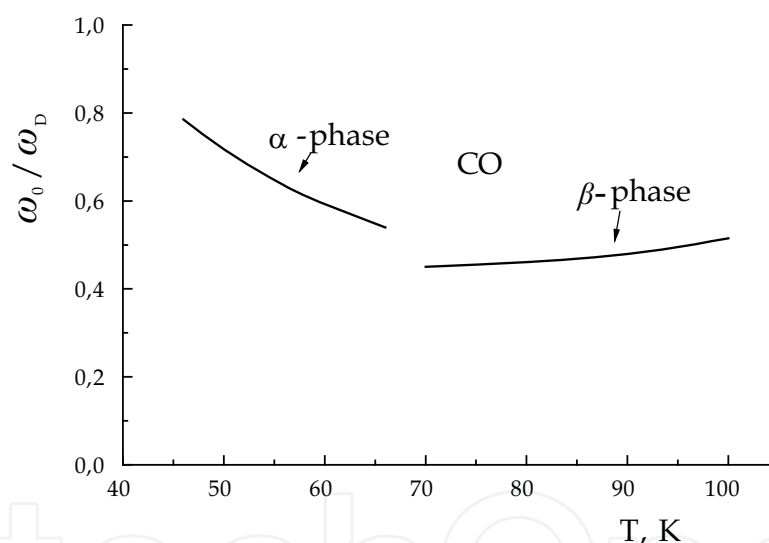

Fig. 16. The ω_0/ω_D ratio upon temperature.

It is seen that near *T=45K* most of the heat is transported by the phonons (the contribution of the "diffusive" modes is no more than *10%*). However, immediately before the *a→β* transition over half of the heat is transported by the "diffusive" modes. In the orientationally-disordered phase the contribution of the "diffusive" modes immediately after phase transition is about two times larger than that of the phonons. As the temperature rises, the contribution of the "diffusive" modes decreases and that of the phonons increases because the scattering of the phonons by the short-range orientational order fluctuations becomes weaker due to their attenuation damping. The estimates show that both three-phonon scattering and one-phonon scattering became the dominant mechanisms. The lower limit of the thermal conductivity is reached when the mean-free paths of all the modes are $\alpha\lambda/2$. It absolutely agrees with Eq. (4) if the polarization-averaged sound velocity $v=(v_l+2v_t)/3$ and $\alpha=1$ are used.
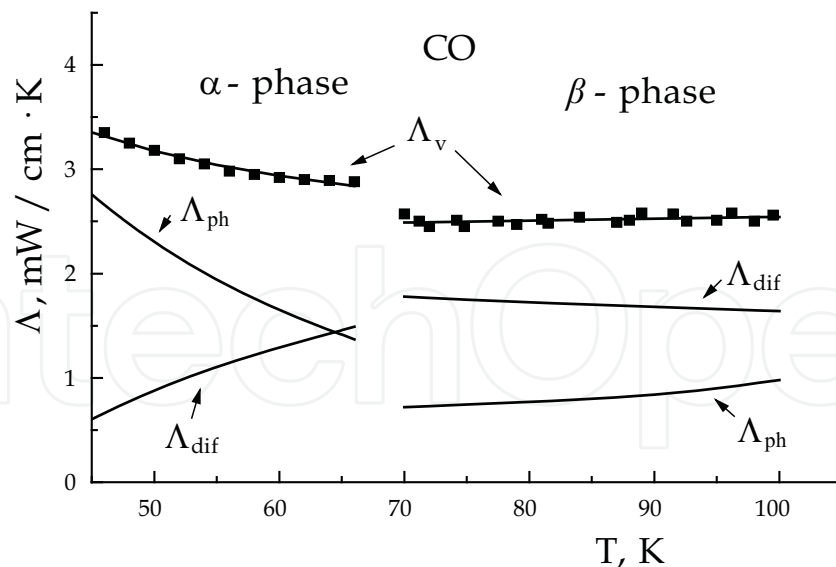
Fig. 17. Results of fitting Λ_V and the contributions to the thermal conductivity of *CO* sample with $V_m=27.93$ *cm³/mole* from low-frequency phonons Λ_{ph} and "diffusive" modes Λ_{dif}.

3.5 Mixed crystals

In the case if thermal conductivity is governed by combined *U*-processes and point defect scattering it follows from Eqs. 8,10 and 21 that

$$\omega_0 = \frac{1}{(2\alpha\pi B)^{\frac{1}{3}}}\left[\sqrt[3]{1+\sqrt{1+u}} + \sqrt[3]{1-\sqrt{1+u}}\right] \tag{28}$$

where

$$u = \frac{4\alpha^2\pi^2 A^3 T^3}{27B} \tag{29}$$

The appropriate contributions to the thermal conductivity from the low-frequency phonons Λ_{ph} and the high-frequency "diffusive" modes Λ_{dif} are

$$\Lambda_{ph} = \frac{k_B}{2\pi^2 \mathrm{v}} \frac{1}{\sqrt{ATB}} arctg\sqrt{\frac{B}{AT}}\omega_0 \tag{30a}$$

$$\Lambda_{dif} = \frac{\alpha k_B}{4\pi \mathrm{v}}(\omega_D^2 - \omega_0^2) \tag{30b}$$

Fig. 18 presents the relative low-frequency phonon contribution Λ_{ph}/Λ to the thermal conductivity of pure *Kr* and the $(CH_4)_{1-\xi}Kr_\xi$ solid solution. A gradual transition from the thermal conductivity of a highly perfect crystal to the "lower limit" to thermal conductivity Λ_{min} was observed at $T\geq\Theta_D$ in the $(CH_4)_{1-\xi}Kr_\xi$ solid solution as the crystal becomes increasingly more disordered. It is seen that in *Kr* the thermal conductivity is of pure phonon character up to about 90*K*. As the *CH₄* concentration increases, progressively more heat is transferred by the "diffusive" modes, but even at the highest concentration (29% of

CH₄ in *Kr*) and the highest temperatures (150*K*) an appreciable part of the heat (about 10%) is transferred by the low-frequency phonons. The values of α vary from 1 to 1.4. This supports the view about the vibrations localized in the $\lambda/2$ regions as the limiting case of the phonon picture (Cahill, 1992) and validity of Eq. (4) for prediction of the lower limit to the thermal conductivity of crystalline lattice. The ω_0/ω_D ratio decreases with rise of temperature and concentration of impurity *CH₄* in *Kr*.
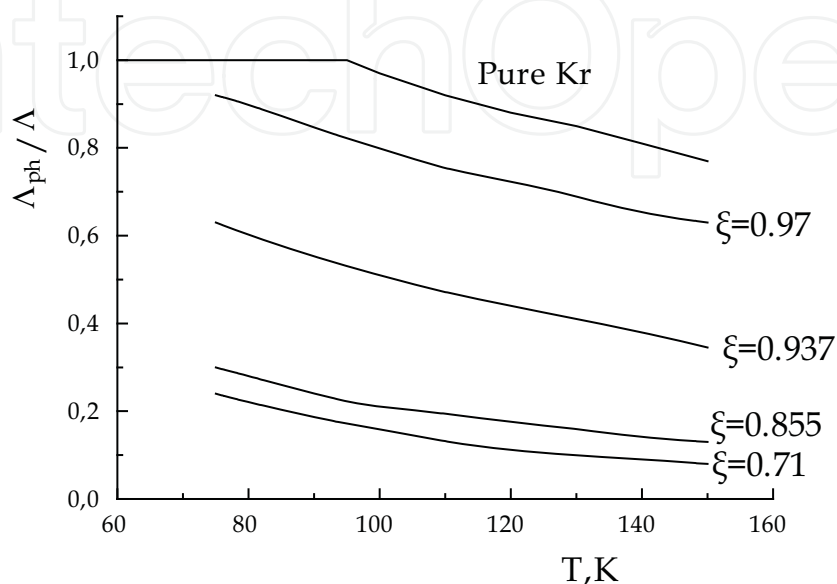
Fig. 18. The relative low-frequency phonon contribution to the thermal conductivity of pure *Kr* and *(CH₄)₁₋ξKrξ* solid solution.

3.6 The Bridgman coefficient *g* and molar volume dependence of thermal conductivity.

Subsequent studies of the thermal conductivity as a function of pressure (Ross et al., 1984) and as a function of density (Konstantinov et.al., 1988-2010) for a wide range of substances have shown that the values of the Bridgman coefficient vary, as a rule, in a range from 3–4 to 10–15. The general tendency is for *g* to decrease with increasing structural disorder; the weakest volume dependence of the thermal conductivity is found in glasses and polymers. In three cases—the *Ih* phase of ice, the phase *NH₄F (I)*, and *CuCl*—the Bridgman coefficient is negative. This is explained by anomalous behavior of the transverse modes, the velocity of which decreases with increasing pressure.

Values of the Bridgman coefficient *g*, measured at temperature *T* for some molecular substances are shown in Tab. 3. The problem of determining the Bridgman coefficient *g* in the present model reduces to finding the volume derivative of the expressions for Λ_{ph} and Λ_{dif}. Since $(\partial ln\Lambda/\partial lnV)_T = 3\gamma+2q-2/3$ we obtain

$$g = \frac{\Lambda_{ph}}{\Lambda}g_{ph} + \frac{\Lambda_{dif}}{\Lambda}g_{dif},\tag{31}$$

where

$$g_{ph} = 5\gamma + 4q - 1,\tag{32a}$$

$$g_{dif} = -\left(\frac{\partial \ln \Lambda_{dif}}{\partial \ln V}\right)_T = -\gamma + \frac{1}{3} + \frac{2}{\omega_D^2 - \omega_0^2}(\omega_D^2\gamma - \omega_0^2\gamma_0), \tag{32b}$$

$$\gamma_0 = 3\gamma + 2g - 1/3, \tag{33}$$

Substance	T, K	g	Substance	T, K	g
Ar	90	9.7	HMT	300	8.9
Kr	120	9.4	Adamantane	320	6.4
Xe	160	9.2	Adamantane	300	9.8
CO_2	220	6.2	Cyclohexane	273	5.5
N_2O	180	5.7	Naphthalene	300	8.5
$\alpha\text{-}N_2$	35	6.0	Anthracene	300	8.9
$\beta\text{-}N_2$	60	4.3	Sulphure	300	6.0
$\alpha\text{-}CO$	60	5.2	$NH_4Cl\ (II)$	298	-6.2
$\beta\text{-}CO$	70	4.0	$NH_4Cl\ (III)$	160	8.6
$\gamma\text{-}O_2$	55	3.8	$NH_4F\ (I)$	298	-6.2
$CH_4\ (I)$	90	8.8	$NH_4F\ (II)$	380	7.5
$CCl_4\ (Ib)$	250	5.8	$NH_4F\ (III)$	386	18
$CCl_4\ (II)$	225	6.5	$H_2O\ (Ih)$	120	-3.9
$CBr_4\ (I)$	360	3.4	$H_2O\ (VII)$	286	4.8
$CBr_4\ (II)$	300	3.8	$H_2O\ (VIII)$	246	4.8
CHF_3	118	4.6	C_2H_6	88	5.5
$CHCl_3$	210	3.9	C_2F_6	170	4.5
CH_2Cl_2	175	4.6	C_3H_8	85	7.5
CF_2Cl_2	115	5.0	C_6H_{14}	178	7.6
$CHF_2Cl(I)$	115	4.5			
C_6H_6	273	7.5			
$SF_6\ (I)$	220	5.2			

Table 3. Values of the Bridgman coefficient g, measured at temperature T.

In our opinion, Eq. 31 has a general character. The main idea pursued in this paper is that the contributions to the molar volume dependence of the thermal conductivity from acoustic phonons and "diffusive" modes are sharply different. If the heat is transferred mainly by acoustic phonons (perfect crystals), then the Bridgman coefficient is described by Eq. 3. In the opposite case, when the thermal conductivity has reached its lower limit Λ_{min} and all the heat is transferred by "diffusive" modes (amorphous solids and strongly disordered crystals), then for $T > \Theta_D$ the lower limit to the thermal conductivity is described by $\Lambda_{min} \propto v/a^{2/3}$, and

$$g = \gamma + 1/3 \tag{34}$$

This also follows from Eq. 32b in the limit $\omega_0 \to 0$. In the general case the Bridgman coefficient g is a weighted average over the acoustic and "diffusive" modes. Fig. 18 shows the Bridgman coefficients calculated for CO_2 and N_2O according to Eqs. 31-33. The temperature dependence of g was not investigated experimentally. For CO_2 and N_2O the Bridgman

coefficients were determined only at the triple-point temperature. It is seen in Fig. 19 that the agreement between the experimental and computed values of *g* is completely satisfactory. It was also found for a number of molecular crystals and their solutions (Konstantinov et al., 2002b, 2003b).
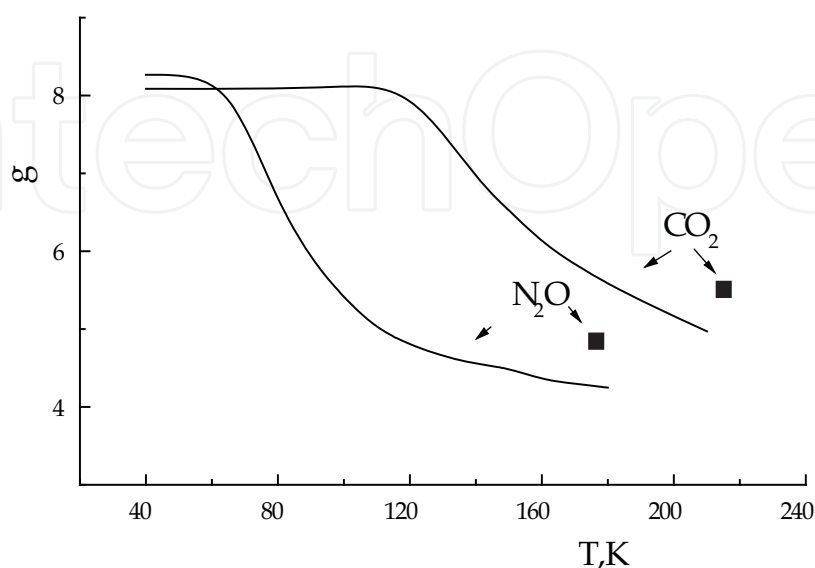

Fig. 19. Temperature dependence of the Bridgman coefficient *g* for solid CO_2 and N_2O calculated according to Eqs. 31-33. Dark squares are experimental values (Konstantinov et al., 1988b).

3.7 Lower limit to thermal conductivity and rotational energy transfer

It was found that the values of coefficient α for molecular crystals, which express the ratio of the lower limit to thermal conductivity obtained by fitting procedure to Λ_{min} calculated from Eq. 4 vary from 2 to 4 (Konstantinov et al., 2003). These values are much larger than for solidified inert gases, where α lies in the range 1.2-1.4. The most obvious reason for this difference is that the site-to-site rotational energy transfer must be taken into account. Eq. 4 for the lower limit of the thermal conductivity is valid for substances consisting of atoms other than molecules with rotational degrees of freedom. Slack, 1979 has taken into account the possibility of thermal energy transfer by optical phonons in crystals consisting of atoms of different kinds. In molecular crystals heat is transferred by mixed translational–orientational modes, whose specific heat for $T{\geq}\Theta_D$ saturates in proportion to the number of degrees of freedom. On this basis the following expression can be suggested for the lower limit of the thermal conductivity of molecular crystal Λ^{*}_{min} whose molecules have z rotational degrees of freedom.

$$\Lambda^{*}_{min} = \frac{1}{2}\left(\frac{\pi}{6}\right)^{1/3}\left(1+\frac{z}{3}\right)k_B n^{2/3}(v_l + 2v_t)\,, \tag{35}$$

It should be noted that although the Eq. 4 for Λ_{min} describes well, over all, the thermal conductivity of amorphous substances and strongly disordered crystals, it is nonetheless semi-empirical. The assumption that the minimum phonon mean-free path length is equal to half the wavelength is only one of many possibilities. Thus, Slack, 1979 assumed that it is

equal to the phonon wavelength. In addition, the expression was obtained on the basis of a very simple Debye model which neglects phonon dispersion and the real density of states. The coefficient α is in such an event an integral factor that effectively takes account of the imperfection of the model.

3.8 Further problems

Up to now there is no consistent theory, describing thermal conductivity of molecular crystals from first principles proceeding from parameters of crystalline potential. Such description is only available for solid methane and deuteromethane (Yasuda, 1978). There is no absolute confidence that semi-empirical approach of Manzhelii et al., 1968 is completely adequate for describing of the thermal conductivity increase with rise of temperature in the case of hindered rotation of molecules, particularly in the case of one-axis rotation. Is there a clearly defined relationship between the frequency of molecular reorientations and the behavior of thermal conductivity?

What is the value of the lower limit to thermal conductivity in molecular crystals? Is there a need to allow for the site-to-site rotational energy transfer? There are not enough arguments for benefit of adequacy of Eq. 35 for describing the lower limit to thermal conductivity in molecular crystals.

There is a lack of data about the temperature dependence of Bridgman coefficient g in the wide temperature range to compare it with calculated values in the framework of the proposed model.

4. References

Auerbach, A. & Allen P.B., (1984). Universal high-temperature saturation in phonon and electron transport. *Physical Review B.*, Vol. 29, No. 6, pp. 2884-2890.

Batchelder, D.N. (1977). In *Rare Gas Solids.* Eds. Klein, M.L.; Venables, J.A., London, New York, San Francisco: Academic Press, Vol. II, 1977, pp. 883-920.

Berman, R. (1976). *Thermal Conduction in Solids*, Clarendon Press, Oxford (1976).

Bondarenko, A.I.; Manzhelii, V.G.; Popov, V.A.; Strzhemechnyi, M.A. & Gavrilko V.G. (1982). Isochoric thermal conductivity of crystalline *Kr* and *Xe*. Heat transfer by vacancies. *Soviet Journal Fizika Nizkikh Temperatur*, Vol. 8, No. 11, pp. 1215-1224.

de Bour, J. (1948). Quantum theory of condensed permanent gases I. Quantum-mechanical low of corresponding states. *Physica*, Vol. 14, No 1, pp. 139–148.

Briels, W.J.; Jansen, A.P.J. & van-der Avoird A. (1985). Translational-rotational coupling in strongly anharmonic molecular crystals with orientational disorder, *Chemie Physics et de Physico-Chemical Biologique*, Vol. 82, No. 2-3, pp. 125-136.

Cahill, D.G.; Watson, S.K. & Pohl R.O., (1992). Lower limit to thermal conductivity of disordered crystals. *Physical Review B.*, Vol. 46, No. 10, pp. 6131-6140.

Clayton, F. & Batchelder, D.N. (1973). Temperature and volume dependence of the thermal conductivity of solid argon. *Journal of Physics. C.*, Vol. 6, No. 7, pp. 1213-1228.

Ecsedy, D.J. & Klemens, P.G. (1977).Thermal resistivity of dielectric crystals due to four-phonon processes and optical modes. *Physical Review B.*, Vol. 15, No. 12, pp. 5957–5962.

Feldman, J.L.; Kluge, M.D.; Allen, P.B. & Wooten F. (1993). Thermal conductivity and localization in glasses: Numerical study of a model of amorphous silicon. *Physical Review B.*, Vol. 48, No. 17, pp. 12589-12602.

Forsman, H. & Andersson, P. (1984). Thermal conductivity at high pressure of solid odd numbered *n*-alkanes ranging from C_9H_{20} to $C_{19}H_{40}$. *Journal of Chemical Physics*, Vol. 80, No. 6, pp. 2804-2807.

Gorodilov, B.Ya.; Korolyuk O.A.; Krivchikov, A.I. & Manzhelii V.G. (2000). Heat Transfer in Solid Solutions Hydrogen-Deuterium. *Journal of Low Temperature Physics*, Vol. 119, No. 3/4, pp. 497-505.

Jeżowski, A.; Stachowiak, P.; Sumarokov V.V., Mucha J. & Freiman, Yu.A. (1993). Thermal conductivity of solid oxygen. *Physical Review Letters*, Vol. 71, pp. 97–100.

Jeżowski A.; Misiorek H.; Sumarokov V.V. & Gorodilov B.Ya. (1997). Thermal conductivity of solid methane. *Physical Review B.*, Vol. 55, No. 9, pp. 5578-5580.

Kawasaki K. (1963). On the behavior of the thermal conductivity near the magnetic transition point. *Progress of Theoretical Physics,* Vol. 29, No 6, pp. 801- 816.

Konstantinov, V.A.; Manzhelii, V.G.; Strzhemechnyi, M.A. & Smirnov, S.A. (1988a). The $\Lambda \propto 1/T$ law and isochoric thermal conductivity of rare gas crystals. *Soviet JournalFizika Nizkikh Temperatur*, Vol. 14, No. 1, pp. 48-54.

Konstantinov, V.A.; Manzhelii, V.G.; Tolkachev, A.M. & Smirnov, S.A. (1988b). Heat transfer in solid CO_2 and N_2O: dependence on the temperature and volume. *Soviet Journal Fizika Nizkikh Temperatur* Vol. 14, No. 2, pp. 412-417.

Konstantinov, V.A.; Manzhelii,V.G. & Smirnov, S.A. (1988c). Isochoric thermal conductivity of solid CO_2 with N_2O and Xe impurities. *Soviet Journal Fizika Nizkikh Temperatur*, Vol. 14, No. 7, pp. 412-413.

Konstantinov, V.A.; Manzhelii, V.G. & Smirnov, S.A. (1991a). Isochoric thermal conductivity and thermal pressure of solid CCl_4. *Physica Status Solidi (b)*. Vol. 163, pp. 368-374.

Konstantinov, V.A.; Manzhelii,V.G. & Smirnov, S.A. (1991b). Isochoric thermal conductivity of solid $CHCl_3$ and CH_2Cl_2. The role of rotational motion of molecules. *Low Temperature Physics*, Vol. 17, No. 7, pp. 462-464.

Konstantinov, V.A.; Manzhelii,V.G. & Smirnov, S.A. (1992a). Temperature dependence of isochoric thermal conductivity of crystalline benzene. *Ukrainian Physical Journal*, Vol. 37, No. 5, pp. 757-760.

Konstantinov, V.A.; Manzhelii,V.G. & Smirnov, S.A. (1992b). Influence of rotational motion of molecules on heat transfer in solid SF_6. *Low Temperature Physics*, Vol. 18, No.11 pp. 902-904.

Konstantinov, V.A. & Manzhelii, V.G. (1994). Phonon scattering and heat transfer in simple molecular crystals. In "*Die Kunst of Phonons*" ed. by T. Paskiewizc, T. Rapsewizc., New York, London: Plenum Press. 1994. pp. 321-332.

Konstantinov, V.A.; Manzhelii, V.G. & Smirnov, S.A. (1995). Isochoric thermal conductivity of solid freons of methane series: CF_2Cl_2 and CHF_2Cl. *Low Temperature Physics*, Vol. 21, No. 1. pp. 78-81.

Konstantinov, V.A.; Manzhelii, V.G.; Revyakin, V.P. & Smirnov, S.A. (1999a). Heat transfer in the orientationally disordered phase of solid methane. *Physica B.* Vol. 262. pp.421-425.

Konstantinov, V.G.; Revyakin, V.P. & Smirnov, S.A. (1999b). A setup for measuring of isochoric thermal conductivity of solidified gases and liquids. *Instruments and Experimental Techniques.* Vol. 42, No. 1, pp. 132-135.

Konstantinov V.A. (1999c). Heat transfer in simple molecular crystals at temperatures of the order of Debye ones and above them. *Functional Materials,*Vol. 6, No. 2, pp. 335–339.

Konstantinov, V.A.; Manzhelii, V.G.; Revyakin, V.P. & Smirnov, S.A. (2000). Manifestation of lower limit to thermal conductivity of solid *Kr* with *CH₄* impurities. *Physica B.*, Vol. 291, pp. 59-65.

Konstantinov, V.A. Manifestation of the lower limit to thermal conductivity in the solidified inert gases. (2001a). *Journal of Low Temperature Physics.* Vol. 122, No. 3/4, pp. 459-465.

Konstantinov, V.A.; Manzhelii, V.G.; Pohl, R.O. & Revyakin V.P. (2001b). Search for the minimum thermal conductivity in mixed cryocrystals $(CH)_{1-\xi}Kr_\xi$. *Low Temperature Physics*, Vol. 27, No. 1. pp. 1159-1169.

Konstantinov, V.A.; Pohl, R.O. & Revyakin V.P. (2002a). Heat transfer in solid $Kr_{1-\xi}Xe_\xi$ solution. *Soviet Physics of Solid State*, Vol. 44, No. 5, pp. 824-829.

Konstantinov, V.A.; Revyakin, V.P. & Orel, E.S. (2002b). Molar volume dependence of thermal conductivity in mixed cryocrystals. *Low Temperature Physics*, Vol. 28, No. 2. pp. 136-139.

Konstantinov, V.A.; Revyakin, V.P. & Orel, E.S. (2003a). Heat transfer by low-frequency phonons and „diffusive" modes in cryocrystal solutions: the *Kr-Xe* system. *Low Temperature Physics*, Vol. 29, No. 9-10. pp. 759-762.

Konstantinov, V.A. (2003b). Heat transfer by low-frequency phonons and „diffusive" modes in molecular crystals. *Low Temperature Physics*, Vol. 29, No. 5. pp. 422-428.

Konstantinov, V.A.; Manzhelii, V.G.; Revyakin, V.P. & Sagan V.V. (2005a). Heat transfer in *γ*-phase of oxygen. *Journal of Low Temperature Physics*, Vol. 139, No. 5-6. pp. 703-709.

Konstantinov, V.A.; Revyakin, V.P.; Manzhelii V.G. & Sagan V.V. (2005b). Isochoric thermal conductivity of solid nitrogen. *Low Temperature Physics*, Vol. 31, No. 5. pp. 419-422.

Konstantinov, V.A.; Manzhelii, V.G.; Revyakin, V.P. & Sagan V.V. (2006a). Isochoric thermal conductivity of solid carbon oxide: the role of phonons and "diffusive" modes. *Journal of Physics*: *Condensed Matter*, Vol. 18, pp. 9901-9909.

Konstantinov, V.A.; Manzhelii, V.G.; Revyakin, V.P. & Sagan V.V. (2006b). Extraordinary temperature dependence of isochoric thermal conductivity of crystalline *CO₂* doped with inert gases. *Low Temperature Physics*, Vol. 32, No. 11, pp. 1076-1077.

Konstantinov, V.A.; Revyakin, V.P. & Sagan V.V. (2006c). Rotation of the methyl groups and thermal conductivity of molecular crystals: ethane. *Low Temperature Physics*, Vol. 32, No. 7. pp. 689-694.

Konstantinov, V.A.; Revyakin, V.P. & Sagan V.V. (2009a). Heat transfer in solid halogenated methanes: trifluoromethane. *Low Temperature Physics*, Vol. 35, No. 4. pp. 286-289.

Konstantinov, V.A.; Revyakin, V.P. & Sagan V.V. (2009b).The isochoric thermal conductivity of solid *n*-alkanes: propane C_3H_8. *Low Temperature Physics*, Vol. 35, No. 7. pp. 577-579.

Konstantinov, V.A.; Revyakin, V.P. & Sagan V.V. (2010). Isochoric thermal conductivity of solid *n*-alkanes: hexane C_6H_{14}. *Low Temperature Physics*, Vol. 36, (in press).

Kokshenev, V.B.; Krupskii I.N. & Kravchenko Yu.G. (1997). High-temperature thermoconductivity of nitrogen-type crystals. *Brazilian Journal of Physics,* Vol. 27, No. 4, pp. 510-514.

Krupski, I.N. & Manzhelii V.G. (1968). Multi phonon interaction and thermal conductivity of crystalline argon, krypton and xenon. *Soviet Journal for Experimental and Theoretical Physics.* Vol. 55, No. 6, pp. 2075-2082.

Krupskii, I.N.; Koloskova L.A. & Manzhelii V.G. (1974). Thermal conductivity of deuteromethane. *Journal of Low Temperature Physics.* Vol. 14, No. 3-4, pp. 403-410.

Lynden-Bell, R.M. & Michel K.H. (1994). Translation-rotation coupling, phase transitions, and elastic phenomena in orientationally disordered crystals. *Review of Modern Physics*, Vol. 66, No. 3, pp. 721-762.

McGaughey, A.J.H. & Kaviany, M. (2004). Thermal conductivity decomposition and analysis using molecular dynamics simulations. Part I. Lennard-Jones argon. *International Journal of Heat and Mass Transfer*, Vol. 47, pp. 1783–1798.

Manzhelii, V.G. & Krupski, I.N. (1968). Thermal conductivity of solid methane. *Soviet Journal Physics of Solids*. Vol. 10, No 1, pp. 284-286.

Manzhelii V.G.; Kokshenev V.B.; Koloskova L.A. & Krupski I.N. (1975). Phonon-libron interaction and thermal conductivity of simplest molecular crystals. *Soviet Journal Fizika Nizkich Temperetur*, Vol. 1, No. 10, pp. 1302-1310.

Manzhelii V.G. & Freiman Yu.A. (1997). In: *Physics of cryocrystals*. Eds. Manzhelii, V.G. & Freiman Yu. A., Woodbury, New York: AIP PRESS. pp. 1-514.

Parsonage, N. & Stavaley, L. (1972). *Disorder in crystals*, Clarendon Press, Oxford.

Pursky, O.I.; Zholonko N.N. & Konstantinov, V.A. (2003). Influence of the rotational motion of molecules on the thermal conductivity of solid SF_6, $CHCl_3$, C_6H_6, and CCl_4. *Low Temperature Physics*, Vol. 29, No. 9/10, pp. 771-775.

Pursky, O.I. & Konstantinov V.A. (2008). Thermal conductivity of solid CHF_2Cl. *Physica B.*, Vol. 403, pp. 190-194.

Purski, O.I.; Zholonko, N.N. & Konstantinov V.A. (2000). Heat transfer in the orientationally disordered phase of SF_6. *Low Temperature Physics*, Vol. 21, No. 1. pp. 278- 281.

Ross, R.G.; Andersson, P.; Sundqvist, B. & Bäckström G. (1984). Thermal conductivity of solids and liquids under pressure. *Report of Progress in Physics*, Vol. 47, pp. 1347–1355.

Roufosse, M.C. & Klemens P.G. (1974). Lattice thermal conductivity of minerals at high temperatures. *Journal of Geophysical Researches*, Vol. 79, No. 5, pp. 703-705.

Sheng, P.; Zhou M. & Zhang Z. (1994). Phonon transport in strong-scattering media. *Physical Review Letters*, Vol. 72, No. 2, pp. 234-237.

Slack, G.A. (1972). In: *Proceedings of International Conference on phonon scattering in solids*, Eds. Albany H.J., Service de documentation du CEN, Saclay, pp. 24-32.

Slack, G.A. (1979). The thermal conductivity of nonmetallic crystals. *Solid State Physics*. Vol. 34, pp. 1-71.

Stachowiak, P.; Sumarokov V.V.; Mucha J. & Jezowski A. (1994). Thermal conductivity of solid nitrogen. *Physical Review B.*, Vol. 50, No. 1, pp. 543-546.

Yasuda H. (1978). Thermal conductivity of solid CH_4 and CD_4. *Journal of Low Temperature Physics*, Vol. 31, No. 1/2, pp. 223-256.
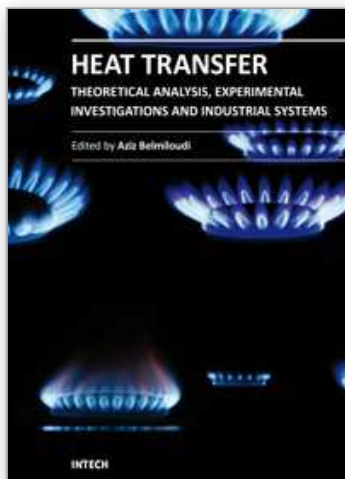
Heat Transfer - Theoretical Analysis, Experimental Investigations and Industrial Systems

Edited by Prof. Aziz Belmiloudi

Over the past few decades there has been a prolific increase in research and development in area of heat transfer, heat exchangers and their associated technologies. This book is a collection of current research in the above mentioned areas and discusses experimental, theoretical and calculation approaches and industrial utilizations with modern ideas and methods to study heat transfer for single and multiphase systems. The topics considered include various basic concepts of heat transfer, the fundamental modes of heat transfer (namely conduction, convection and radiation), thermophysical properties, condensation, boiling, freezing, innovative experiments, measurement analysis, theoretical models and simulations, with many real-world problems and important modern applications. The book is divided in four sections : "Heat Transfer in Micro Systems", "Boiling, Freezing and Condensation Heat Transfer", "Heat Transfer and its Assessment", "Heat Transfer Calculations", and each section discusses a wide variety of techniques, methods and applications in accordance with the subjects. The combination of theoretical and experimental investigations with many important practical applications of current interest will make this book of interest to researchers, scientists, engineers and graduate students, who make use of experimental and theoretical investigations, assessment and enhancement techniques in this multidisciplinary field as well as to researchers in mathematical modelling, computer simulations and information sciences, who make use of experimental and theoretical investigations as a means of critical assessment of models and results derived from advanced numerical simulations and improvement of the developed models and numerical methods.

How to reference

In order to correctly reference this scholarly work, feel free to copy and paste the following:

INTECH
open science | open minds

www.intechopen.com

Phone: +385 (51) 770 447
Fax: +385 (51) 686 166
www.intechopen.com

Phone: +86-21-62489820
Fax: +86-21-62489821